1989

Design., analysis and experiment planning of one-story reinforced concrete frame-wall-diaphragm assemblage, July 1989

Kai Yu

Ti Huang

Le-Wu Lu

514.2

DESIGN, ANALYSIS AND EXPERIMENT PLANNING OF ONE-STORY REINFORCED CONCRETE FRAME-WALL-DIAPHRAGM ASSEMBLAGE

by

Kai Yu ,Ti Huang and Le Wu Lu

Department of Civil Engineering

Fritz Engineering Laboratory

Lehigh University

Bethlehem, Pennsyvania

July 1989

Table of Contents

List of Figures

List of Tables

Acknowledgement

The work presented in this report was a part of a research project, "Seismic Response of Building Structure with Flexible Floor Diaphragms", conducted jointly at Lehigh University and the State University of New York at Buffalo (SUNY/Buffalo). The project is funded by the National Center for Earthquake Engineering Research headquartered at SUNY/Buffalo. The center is supported by the National Science Foundation and the State of New York.

Professor Andrei M. Reinhorn and Dr. Nader Panahshahi, the investigators at SUNY/Buffalo, are gratefully acknowledged for their valuable cooperation in this study.

Abstract

A cooperative research project studying effect of floor diaphragm flexibility on seismic responses of building structure has been carried out at Lehigh University and the State University of New York at Buffalo (SUNY/Buffalo). An one-story one-sixth scale reinforced concrete structure consisting of shear walls, frames and floor diaphragms has been developed to be the test structure for this study.

In the design of the test structure, the behavior of an one-story prototype reinforced concrete structure was studied first. The internal forces of the prototype structure were then scaled down to the model dimension. Finally, based on the scaled internal forces, the model test structure was designed in accordance with ACI Code (318-83) and its Appendix A. In order to meet the similitude requirements for dynamic response, an ultimate strength modelling method with artificial mass simulation was adopted in the design. The modelling of the model materials was undertaken with the purpose of making a test structure possessing large ductility under seismic loads.

The static and dynamic characteristics of the model assemblage and its three components, shear wall, frame and slab, are studied elastically and inelastically by computer program analysis. The diaphragm action of the slab on the distribution of lateral loads among the shear walls and frames is examined in detail ad different levels of earthquake ground motion inputs.

The complete assemblage structure will be tested on the shaking table at SUNY/Buffalo. Prior to the test, three individual components (shear wall, frame and slab) will be tested cyclically at Lehigh University, the results of which will be used to develop predictions of the dynamic response. In

addition, an identical assemblage model will be tested cyclically at Lehigh University. The test setups and instrumentation for the component and assemblage tests have been designed to perform a series of proposed tests.

Chapter 1
Introduction

Floor slabs are used in multi-story buildings to serve many important structural functions. They not only transmit the gravity loads to the vertical structural systems, such as frames and shear walls, but also act integrally with the vertical systems in resisting lateral as well as gravity loads. The primary action of the slabs for these two functions is out-of-plane bending, a problem which has been studied extensively. The analytical tools necessary to predict out-of-plane slab behavior are readily available.

Distribution of lateral loads to parallel vertical structural systems is another important function of the floor slabs. When a building is subjected to a severe earthquake, the inertial forces generated in the floor slabs must be transferred to the vertical structural systems through the diaphragm action of the slabs. The performance of the diaphragm action of the floor slab is controlled primarily by its in-plane stiffness. In many structures, a reasonable estimate of the inertial force distribution can be achieved by assuming that the slabs act as rigid diaphragms. However, for structures in which the stiffness of the vertical system and the stiffness of the slab system do not differ greatly, diaphragm deformation of the floors must be explicitly considered in analysis.

There is currently insufficient knowledge to determine whether the rigid-diaphragm assumption will lead to adequate design for a given structure, whether the diaphragm flexibility requires special consideration, and how to define the rigidity of a horizontal diaphragm relative to the stiffness of the vertical lateral load resisting systems. Although the need for such information has been recognized by structural engineers, only a small amount of

analytical and experimental research has been conducted, especially on reinforced concrete diaphragms.

In recent years, research has been carried out to study the in-plane characteristics of reinforced concrete floor diaphragms (8, 9, 13), and approximate analytical models have been proposed for investigating the effect of diaphragm flexibility on seismic building responses (6, 7, 14). The distribution of seismic forces to the vertical structural elements has been found to be very complex, especially after the floor diaphragms have experienced significant cracking and yielding. All available methods of analysis for structures with flexible diaphragms use very simple models to represent the behavior of the various structural elements. Furthermore, the results of those analyses have not been sufficiently verified by tests performed on three-dimensional structures.

An analytical and experimental research program is being conducted on a cooperative basis between Lehigh University and SUNY/Buffalo. The primary objective of the program is to understand the effect of the diaphragm flexibility on the redistribution of lateral forces to the vertical structural system after the floor slab system has experienced inelastic deformation. This is to be achieved by conducting a series of tests on a one story 3D reinforced concrete structure under lateral loads up to collapse load level. The test results will be used to correlate with analytical predictions and to develop specific procedures for the analysis of inelastic building systems including the effect of in-plane slab flexibility.

The study presented here is part of the joint research program and includes the following tasks:

- Design of a one-sixth scale model test structure for both dynamic (shaking table) and quasi-static tests.
- Predication of the lateral load behavior of various components

and the total assemblage of the model structure .

- Modelling concrete and reinforcement of the model structure.
- Planning of quasi-static tests of the model components and the model structure.

The test results of the three components and the model assemblage structure and the corelation with theoretical predictions will be presented in separate reports.

Chapter 2
Design of the Model Structure

2.1 Description of the Test Structures

The one-story one-sixth scale reinforced concrete test structure selected is intended to represent the lower part of multistory building. Obviously, it would be ideal to test a multistory, multi-bay building structure specimens, with lateral motions in both horizontal directions, in order to examine the overall diaphragm effect of the slab systems. However, on account of the budgetary constraint, and the limited capacity of the shaking table at SUNY/Buffalo, only a one-story structure could be studied.

2.1.1 Model Assemblages

The small-scale model structure chosen for the experimental study is an assemblage one story high, one bay deep and four bays long, with a coupled shear wall at each end, and three intermediate frames. The model dimensions were chosen to represent a one-sixth scale model of the lower part of a multistory prototype structure. The story height is 36 in.. The slab panels are 1.17 in. thick, and 48 in. square, with 8 in. extensions beyond the column and wall center lines. The extensions are intended to simulate the effect of continuous slab panels in neighboring bays in the prototype structure. The model columns are 3 in. square. The beam stems below the slab in both directions are 2.5 in. deep and 2 in. wide. The twin shear walls are 20 in. x 2 in. in cross section, and connected by a linking beam 24 in. long. The detail dimensions of the model assemblage are given in Fig. 2-1. The details of the model assemblage structures for the dynamic tests on the shaking table at SUNY/Buffalo and for the quasi-static tests at Lehigh University are identical. The prototype structure has the same configuration

with linear dimensions six times larger.

2.1.2 Model Components

In order to facilitate predictions of the behavior of the model assemblage structure under both the dynamic and quasi-static tests, three component structures, including a coupled shear wall, an isolated transverse frame and a single slab panel (Figs. 2-2, 2-3 and 2-4), will be statically and cyclically tested up to ultimate strength at Lehigh University beforehand. The design details of each of the components are identical to the corresponding portion in the model assemblage.

For the frame and the shear wall component structures, a 20 in. wide slab strip is included. According to Section 13.2.4 of ACI 318-83 (1), the effective flange width of the transverse beam is only 7 in. However, such small slab width would lead to considerable difficulty in the application of supplemental gravity load (refer to Section 2.3). Analytical study of the assemblage structure by SAP-IV (3) revealed that under gravity load, the lines of zero longitudinal bending moments were approximately 20 in. apart. This width was adopted for the slab portion on the shear wall and frame component specimens. Both the application of supplemental gravity load and the simulation of inertial force boundary conditions at the slab edges are greatly simplified, since only shear force exists on the edges (Figs. 2-2, 2-3). The slab panel component specimen has total dimensions of 58 in. x 64 in., with the two transverse beams enlarged for the purpose of connecting to the support and loading fixtures. The design detail of the slab component is identical to that of the middle panels of the model assemblage structure.

2.2 Aspects of The Design of The Model Assemblage and The Components

2.2.1 Initial Considerations

As indicated earlier, a one-story shear-wall-frame-slab assemblage has been selected as the testing structure, instead of a more complete structure. At the beginning, it was intended to design the specimen as a part of a multistory structure. However, the similitude requirements of gravity loading, the structural actions of the upper part of the structure and the boundary conditions make such a test model impractical.

After considerable discussion, it was finally decided to design the specimen as a reduced scale model of an one-story prototype structure. The prototype structure was first analyzed for the desired seismic loads as well as live and dead loads. The calculated internal moments and forces were scaled down to the model dimensions, and then the model assemblage was designed for these internal reduced moments and forces. No attempt was made to model individual reinforcing bars of the prototype structure. The model assemblage so designed was then analyzed to determine its behavior under static loads and dynamic earthquake ground motions, both elastically and inelastically.

2.2.2 General Design Criteria and Assumptions

1. The equivalent frame design method described in ACI 318-83 (1) is to be used.
2. The design gravity loads include the dead load corresponding to the weight of the structural members (beams, slabs, columns and shear walls) and a uniform live load of 80 psf.
3. In calculating the design earthquake lateral forces, at least 25% of the floor live load is taken to be present on all panels. This is in line with the UBC (18) requirement.
4. The characteristics of deformed reinforcing bars for the model

are as follows: D2 bars: yield strength 50 ksi; ultimate strength 60 ksi. D1 bars: yield strength 50 ksi; ultimate strength 60 ksi. Deformed G14 bars for slabs: yield strength 40 ksi; ultimate strength 50 ksi. Undeformed G14 bars for lateral reinforcement(stirrups and ties): yield strength 35 ksi; ultimate strength 50 ksi.

5. The characteristics of concrete in the model as well as the prototype are as follows: maximum aggregate size 1/4", unit weight 150 pcf , compressive strength $f_c' = 4000$ psi.

2.2.3 Analysis of The Prototype Assemblage

The prototype one-story shear-wall-frame-slab assemblage is analyzed by the ACI equivalent frame method. For the longitudinal direction, the assemblage structure consists of two identical frames, Frame A, separated by the center line. For the transverse direction, there are three intermediate frames, Frame B, and two unsymmetrical end shear-wall frames (Fig. 2-1).

Two factored load combinations are considered in the analysis of the assemblage structure; 1.4D + 1.7L and 0.75 (1.4D + 1.7L + 1.87E), where D = service dead load, L = service live load, E = seismic load = cW_t, W_t = total gravity service dead load + 25% of live load = D + 0.25L, and c = 0.112 for the longitudinal direction and c = 0.094 for the transverse direction. A calculation of the seismic load is given in detail in Appendix A. It is not necessary to consider wind load for a one story structure.

For the one story assemblage structure considered, only one critical cross section is controlled by seismic loading (Section A in Frame A in Fig. 2-6) All other critical sections were controlled by the gravity loading combination, 1.4D+1.7L. The design of moment envelopes for Frame A and Frame B are shown in Fig. 2-6. In accordance with the ACI Building code, the moments in Frame A computed by the Equivalent Frame Method may be proportionally reduced so that the sum of the absolute values of the positive and negative moments does not exceed the total static moment,

$M_o = w_u L_2 L_n^2/8$, where w_u = factored load per unit area, L_2 = width of equivalent frame and L_n = length of clear span in direction of the moments being determined, measured face-to-face of supports. The critical moments are distributed among beams, column strip slabs and middle strip slab according to the ACI provisions. The results are shown in Tables 2-1 and 2-2.

2.2.4 Final Design of the Model Assemblage And the Components

The critical section moments and forces obtained from the analyses of the prototype structure under gravity and seismic loading are reduced by appropriate scale factors to yield the corresponding moments and forces in the model assemblage structure. For the one-sixth model, the scale factor for moment is $(1/6)^3$ and the scale factor for axial and shear forces is $(1/6)^2$. The required nominal design moment strengths at critical sections in Frame A and Frame B for the model assemblage are listed in Tables 2-3 and 2-4. The conversion of moment values from Tables 2-1 and 2-2 to Tables 2-3 and 2-4 involves not only the scale factor $(1/6)^3$, but also the ϕ factor of 0.9 as well as the factor 12 for the conversion from kip-ft to kip-in. units.

The design of all elements in the model structure (assemblage as well as components) is done in accordance with the ACI 318-83 strength method, including the seismic provision of Appendix A (1). The design of the slab is based on flexural consideration only. The beams and columns are designed for the combined effect of bending, axial, and shear forces (20). However, no consideration is given to the twisting of the beams perpendicular to the direction of seismic loading, induced by the rotation of the longitudinal beam-column joints, which is associated with the sideway deflection of the structure.

The reinforcement details of the component specimens (frames, shear-

walls and slabs) are shown in Figs. 2-7, 2-8 and 2-9. These reinforcing details are identical to those in the corresponding parts of the model assemblage. The beams in the direction of Frame B are referred to as "main beams". The beams in the direction of Frame A are referred to as "longitudinal beams". As shown in Fig. 2-7 and Fig. 2-8, reinforcing bars in the longitudinal beams are placed inside of those in the main beams. Two sizes of deformed reinforcing bars, D1 and D2, are used for beams and columns. The D1 bars, with a diameter of 0.115 in., approximately correspond to #5 bars in the prototype. The D2 bars are 0.163 in. in diameter, and approximately correspond to #8 bars in the prototype. The thickness of concrete cover to the steel in beams is 0.5 in for the longitudinal beams and 0.34 in for the main beams, (Fig. 2-8), corresponding to 3 in. and 2 in. respectively for the prototype. These cover thicknesses are selected to facilitate the placing of concrete in the model. The range of reinforcement ratio for the beams is ρ=0.6%-1.3% based on the web width. The columns have a reinforcement ratio of ρ_g=1.3%. The stirrups in the beams, the ties in the columns and the edge columns of the shear walls, particularly the lateral steel in the beam-column joint areas, are designed as required by Appendix A of ACI 318-83 to prevent shear failure and to ensure adequate ductility in the event of formation of plastic hinges (19).

The reinforcement arrangement in the shear-wall is influenced by the desire to postpone the failure of the shear wall until after the yielding of the middle panel slabs in the model assemblage structure. The strengthening of the shear wall is achieved by adding reinforcing steel at the edges, in effect, forming edge columns or boundary elements, 2 in. x 3 in., in cross section, (see Fig. 2-7). Each edge column contains 14 D1 bars, representing a reinforcement ratio of ρ_g = 1.05%. The body of the shear wall is reinforced

with D1 bars at 1.25 in. spacings vertically and 1 in. spacings horizontally.

Slab reinforcement consists of G14 deformed wires, 0.08 in. in diameter, corresponding to approximately #4 bars for the prototype. The reinforcement arrangements for the two middle slab panels are identical, so are those in the two end panels.

2.3 Requirement of Added Weight on The Model

2.3.1 Simulation of Dead Load

In order to obtain a reliable prediction of the prototype response to dynamic loading, an ultimate strength model with mass simulation is chosen (10). The reinforcing steel and concrete materials are chosen to have the same density and strength values as those used in the prototype structure. However, perfect modelling of the dynamic behavior requires that $\rho_m=\rho_p E_r/L_r$, where ρ_m=mass density of model material, ρ_p=mass density of prototype material, E_r=model to prototype modulus scaling factor, and L_r=model to prototype geometrical scaling factor. If the density and modulus are both maintained at the prototype values, the geometrical scaling factor must be 1, or no dimensional reduction is permissible. A practical solution to this difficulty is to place extra weights on the model structure, effectively increasing its "mass density", while maintaining the modulus of the model materials to be the same as those in the prototype. Thus $E_r=1$, and $\rho_m=\rho_r/L_r$. The additional effective density needed to preserve dynamic similitude is $\rho_m-\rho_p=(1/L_r-1)\rho_p$. For the one-sixth scale model, the additional weight needs to be five times the weight of the model structure in order to satisfy the similitude requirements.

2.3.2 Simulation of Live Load

For the dynamic tests on the shaking table, it is desirable to use as much mass on the model assemblage as possible in order to produce large inertial forces. The mass in the test should reflect not only the weights of the structure, but the effect of live load as well. The Uniform Building Code (UBC) (18) currently requires that for seismic design of a typical office building, 25% of live load should be considered over all the floor area. For the current study, full live load is applied to the two middle panels, while the two end panels are unloaded, resulting in an average of 50% live load. The higher-than-specification live load used is to induce a sufficiently high inertial force in order to bring the structure to its ultimate strength within the limited capacity of the shaking table.

The arrangement of additional weights to simulate the dead and live loads on the model assemblage for the dynamic test at SUNY/Buffalo is shown in detail in Fig. 2-5. For the quasi-static test on the assemblage at Lehigh University, the weights are applied as concentrated loads at the center of each panel. For the component specimens, the additional loads are applied by suspending weights underneath the slabs. The amount of additional weight for each component specimen test depends upon its tributary area of the slab in the model assemblage. The additional weight is 780 Lb for the shear wall specimen, 3780 lb for the frame specimen, and 3800 Lb for the slab specimen. The weight for each component specimen is the same as the additional weight used over the corresponding tributary area in the assemblage for the shaking table test at SUNY/Buffalo.

Table

Table 2-1: Design Moments for the Prototype Structure, Frame A

STRIP	SECTION A	SECTION B	SECTION C & D	SECTION E	SECTION F
Beam	-87.42	79.23	-110.68	67.71	-96.43
Column	-15.43	13.98	-19.53	11.95	-17.17
Middle	-11.15	31.07	-43.41	26.55	-37.82

Unit: kip-ft

Table 2-2: Design Moments for the Prototype Structure, Frame B

STRIP	SECTION A	SECTION B
Beam	-111.44	171.48
Column	-19.67	30.26
Middle	-9.11	67.25

Unit: kip-ft

Table 2-3: Required Nominal Moment Strength for the Model Assemblage Frame A

STRIP	SECTION A	SECTION B	SECTION C & D	SECTION E	SECTION F
Beam	-7.138*	4.891	-6.832	4.180	-5.952
Column	-0.952	0.863	-1.206	0.738	-1.060
Middle	-0.688	1.918	-2.680	1.638	-2.335

Unit: kip-in

* Controlled by combined dead, live and earthquake loading. All other sections controlled by gravity loading.

Table 2-4: Required Nominal Moment Strength for the Model Assemblage Frame B

STRIP	SECTION A	SECTION B
Beam	-6.879	10.585
Column	-1.214	1.868
Middle	-0.562	4.151

Unit: kip-in

Figure

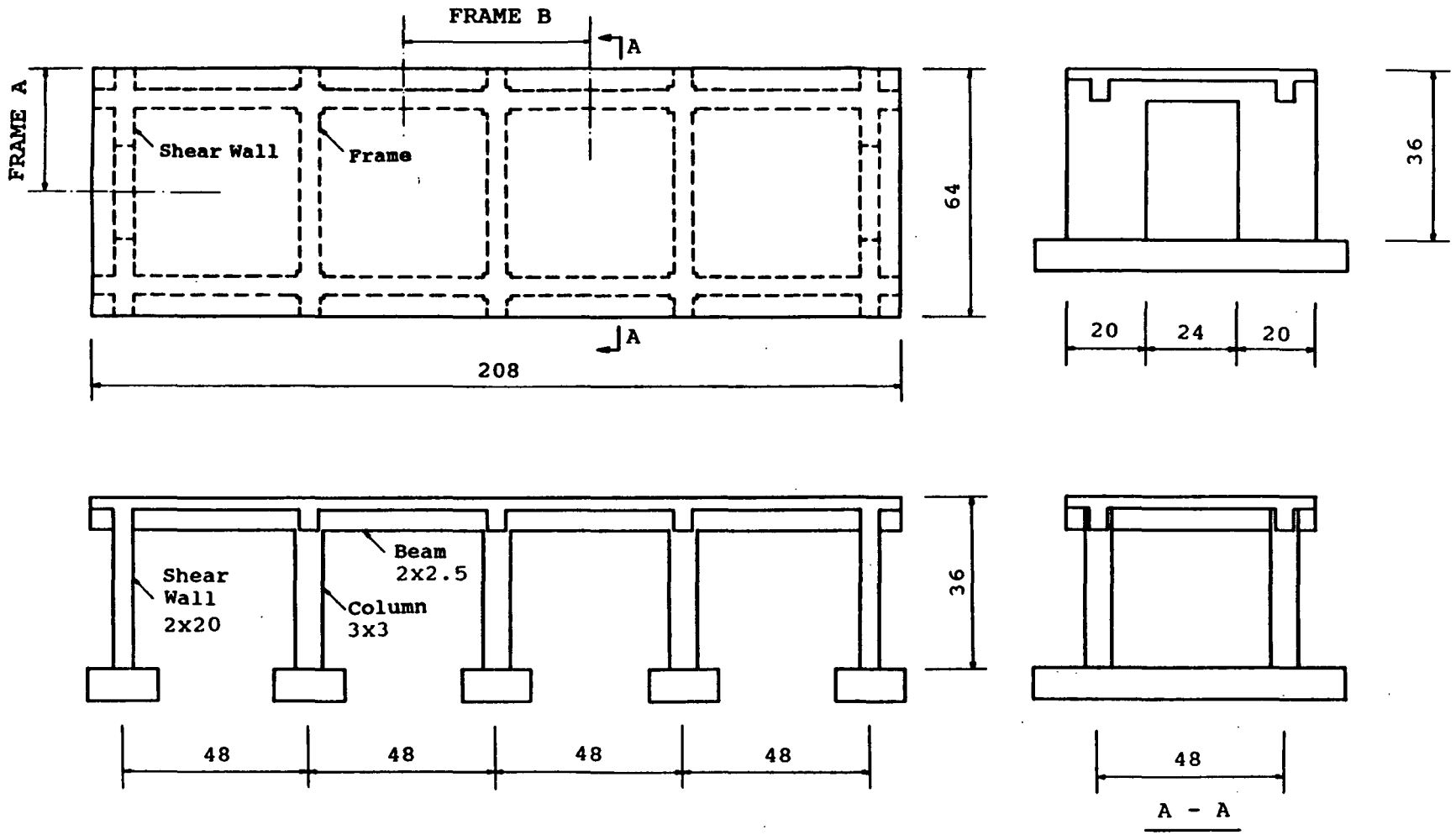

Figure 2-1: Model Assemblage

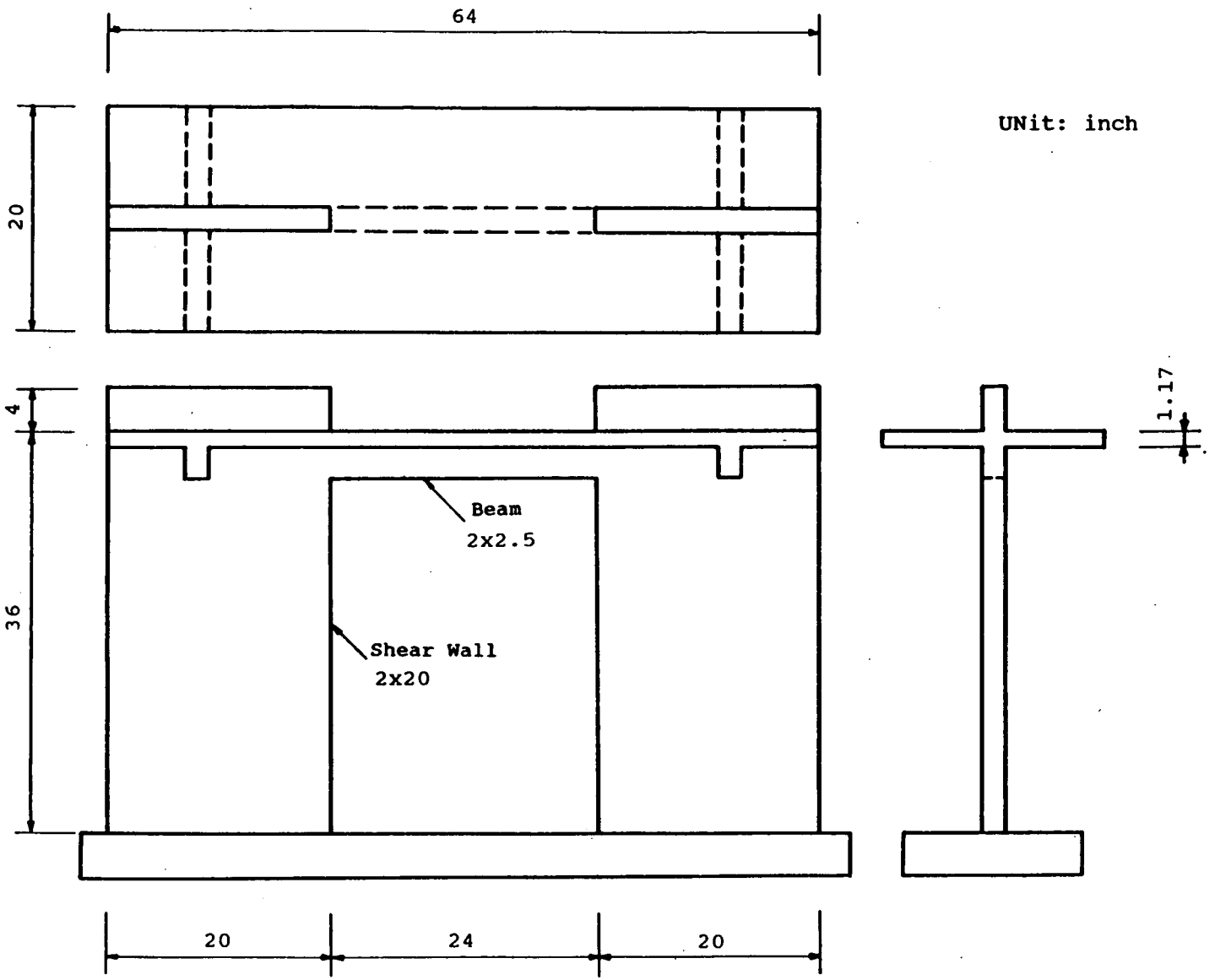

Figure 2-2: Model Shear Wall

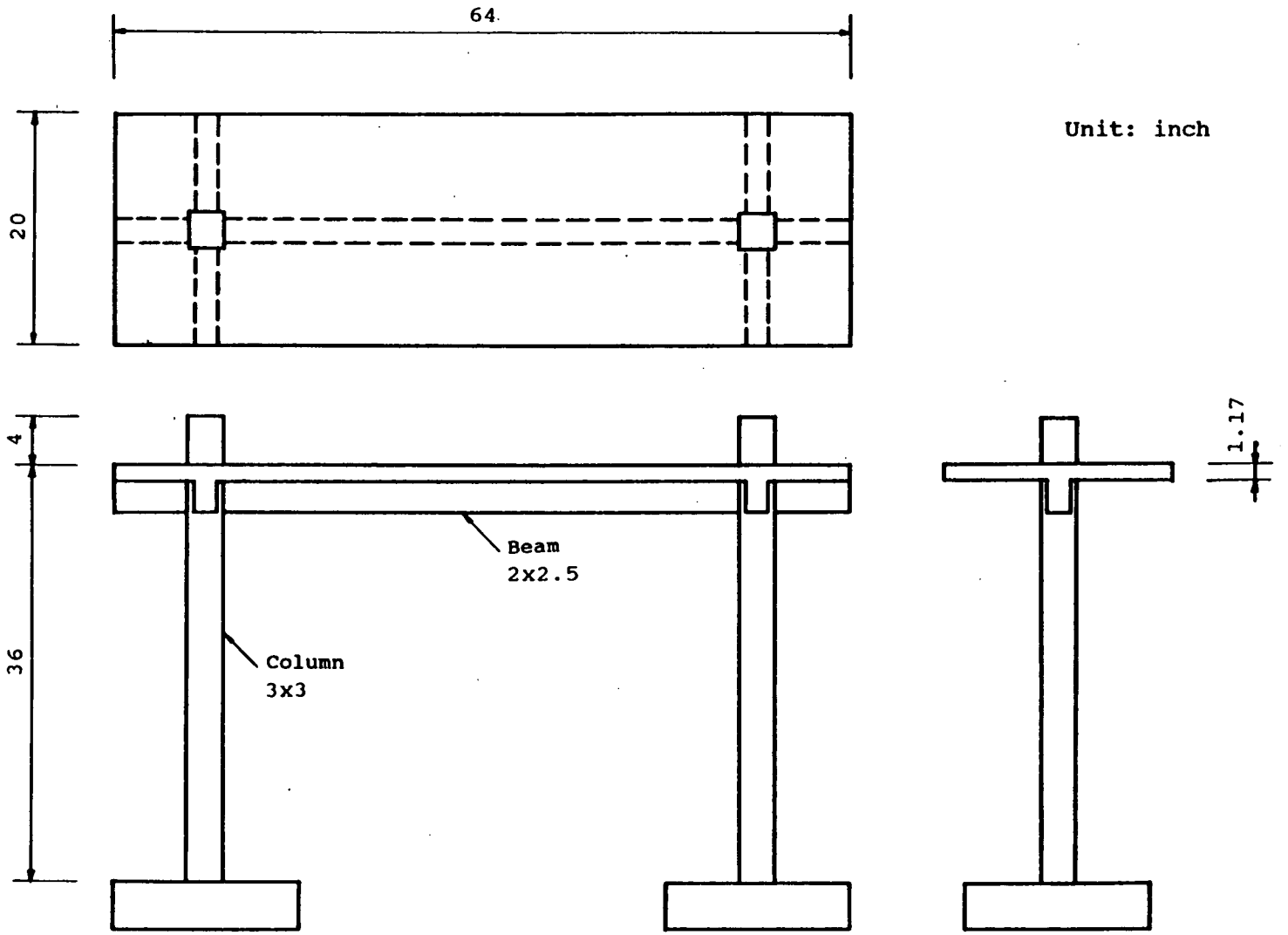

Figure 2-3: Model Frame

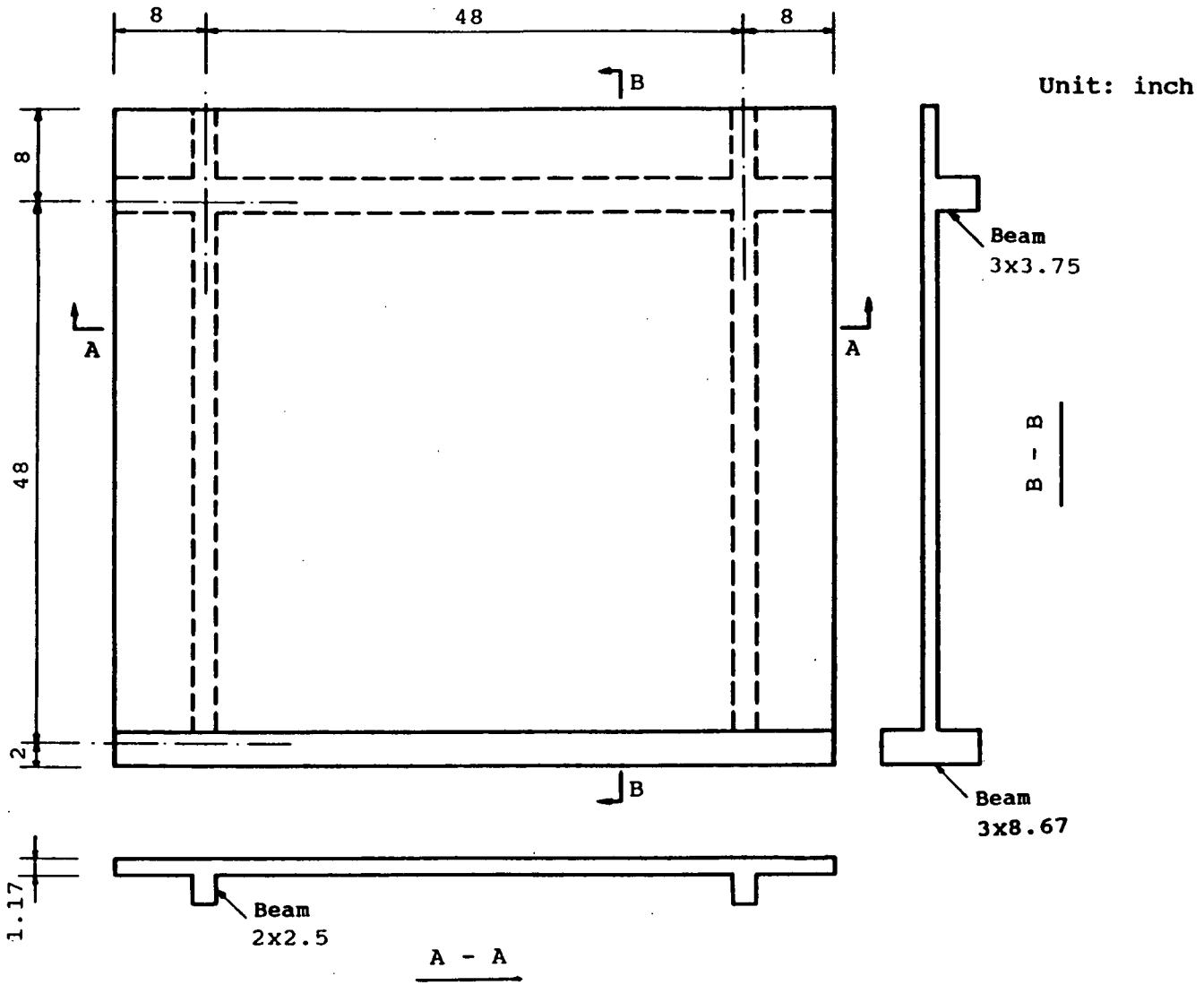

Figure 2-4: Model Slab

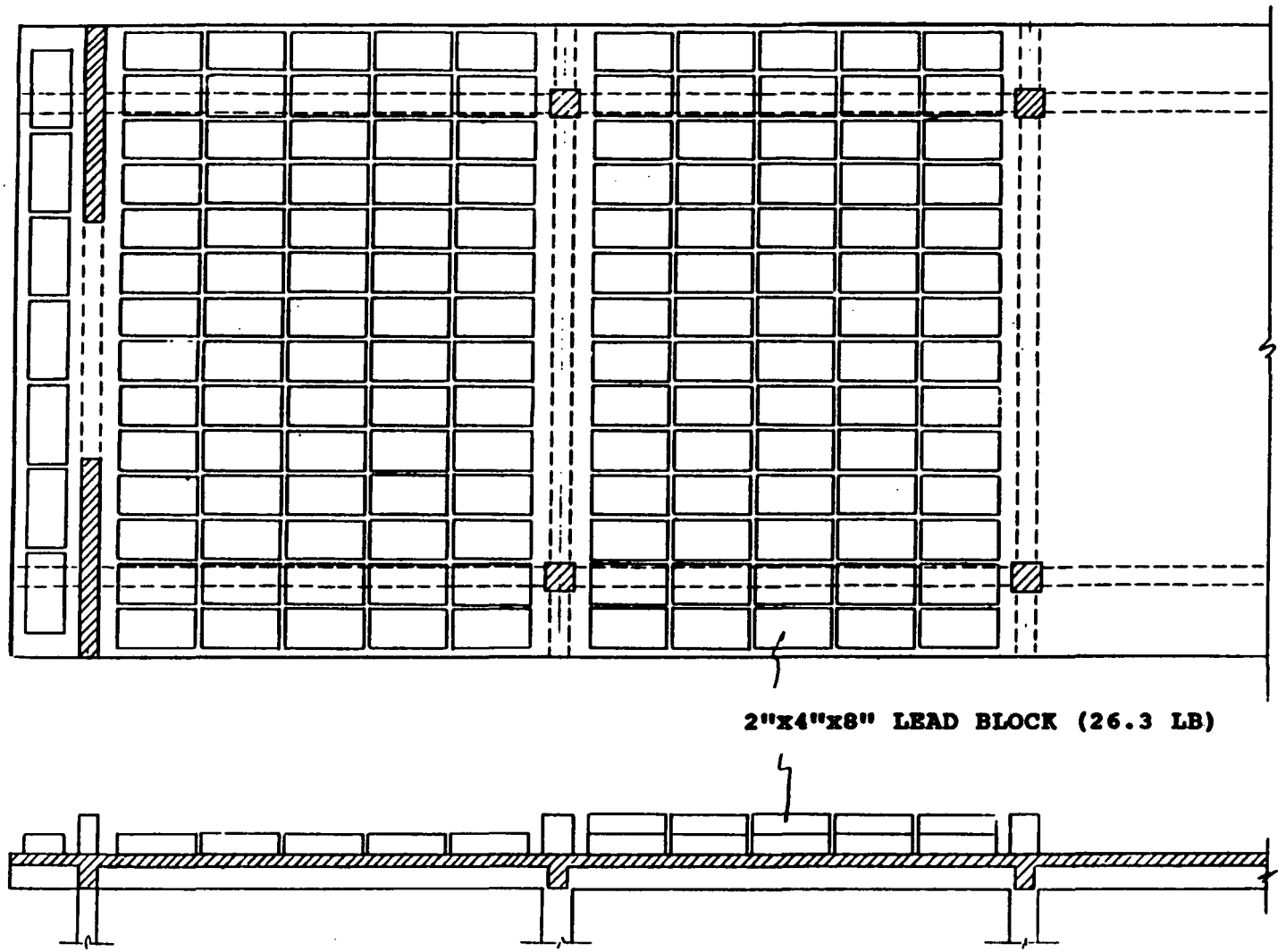

Figure 2-5: Additional Mass for the Model Assemblage

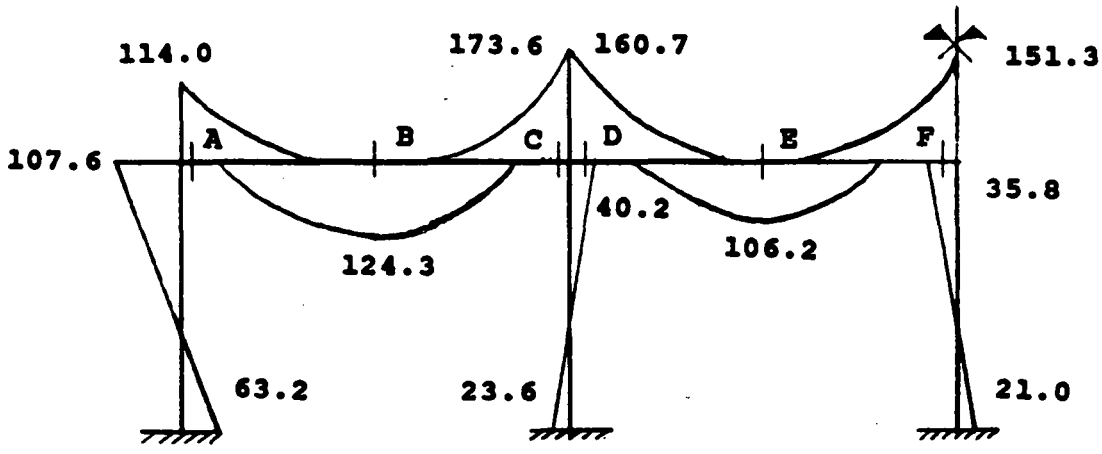

Moment Envelope of Frame A

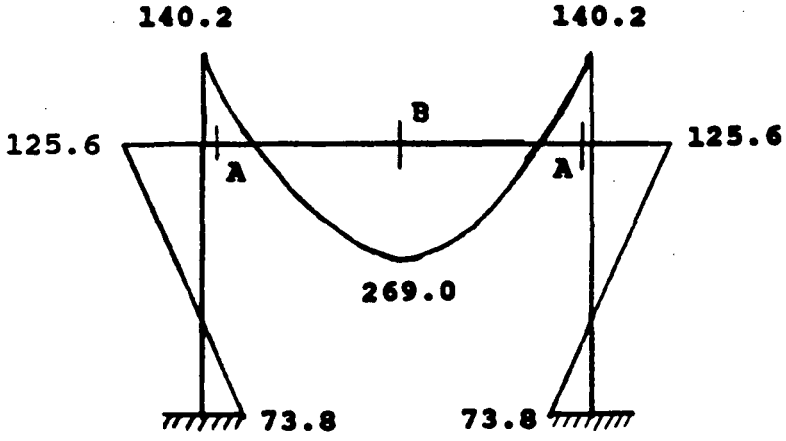

Moment Envelope of Frame B

Figure 2-6: Moment Envelope of the Assemblage structure in Protorype Dimension

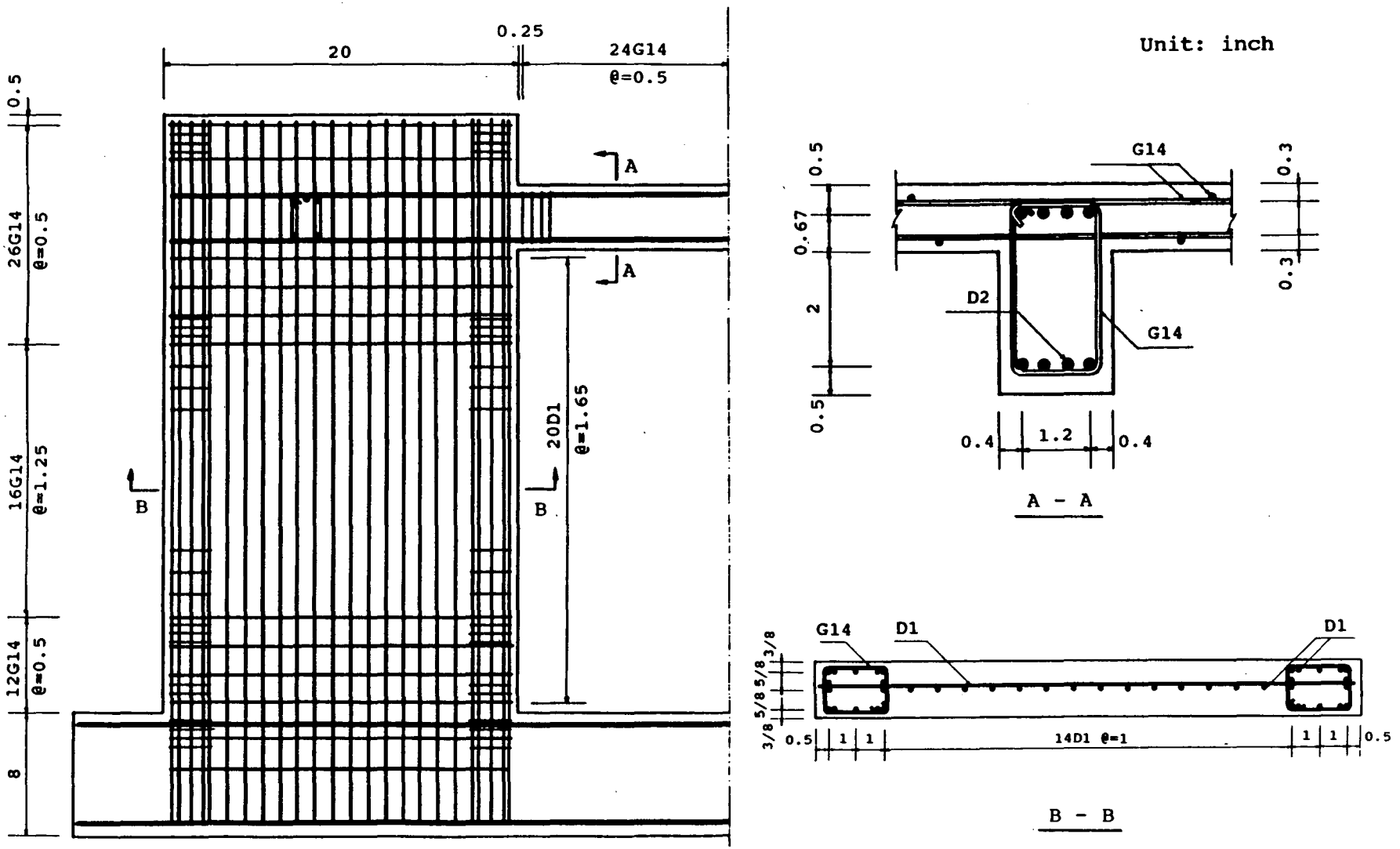

Figure 2-7: Reinforcement for Shear Wall

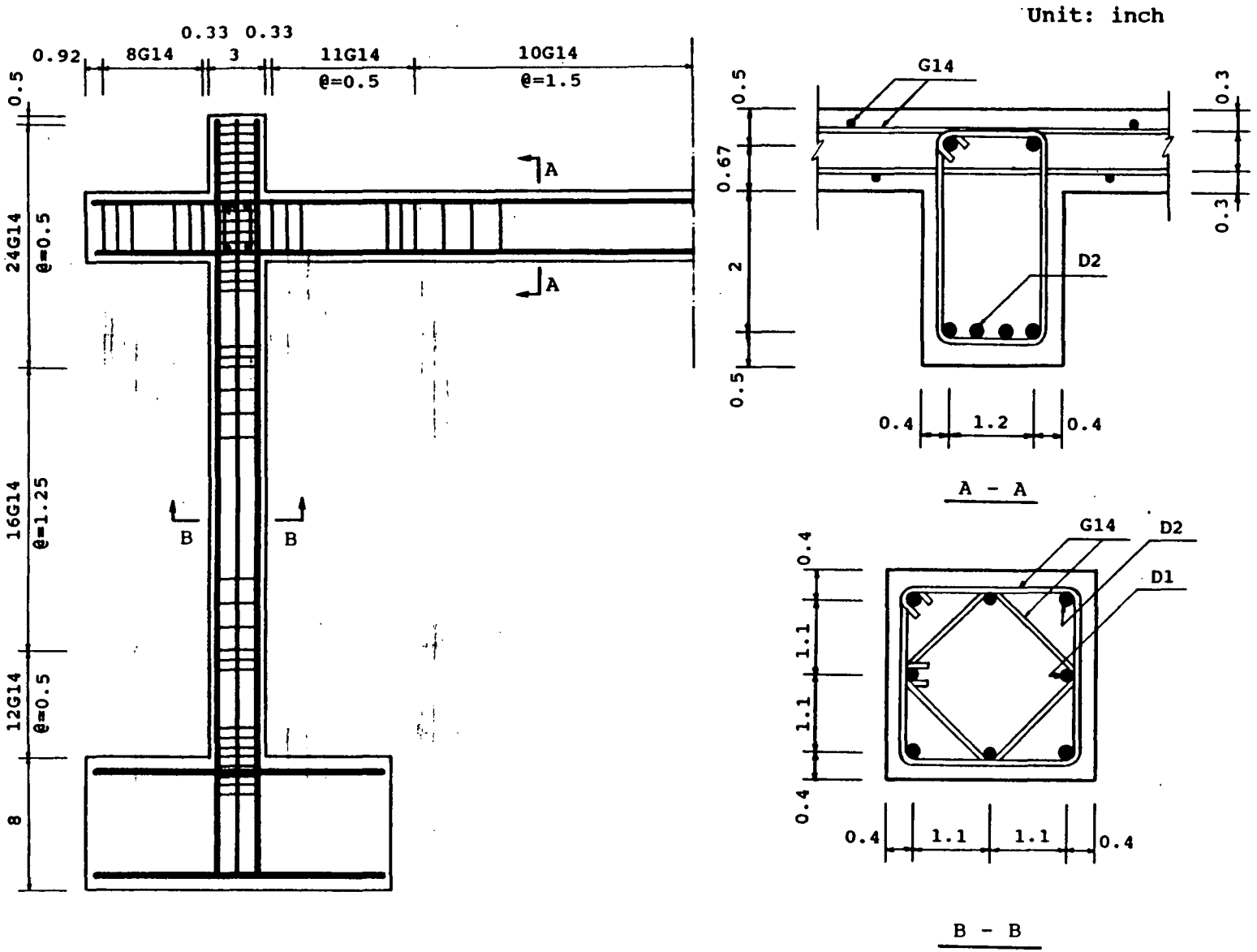

Figure 2-8: Reinforcement for Frame

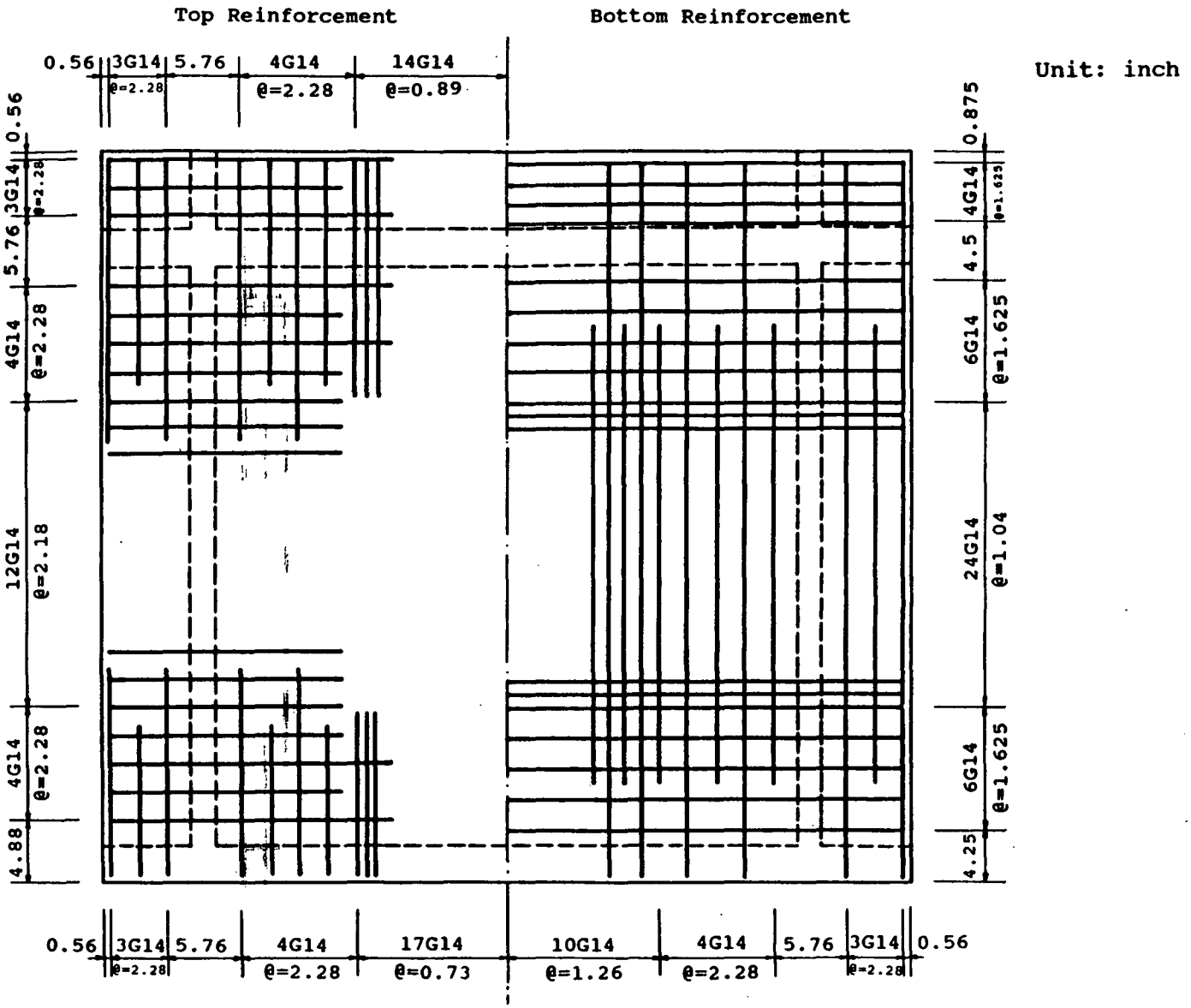

Figure 2-9: Reinforcement for Slab

Chapter 3
Computer Analysis of the Three components and the Model Assemblage

3.1 General

Behavior of a reinforced concrete frame-wall-diaphragm structure is very complex under seismic loads. The situation is even more difficult to predict if the structural response exceeds the limit of linearity and if the diaphragm action of the floor system is included. In most design practice, concrete floor slabs are assumed to have infinite in-plane stiffness and the effect of their out-of-plane bending on the distribution of lateral loads among the vertical lateral force resistant systems is ignored. However, recent experiences have revealed that flexibility of floor diaphragms can be an important factor to the dynamic characteristics of high-rise buildings under seismic action. For example, opening and closing of concrete floor slab cracks may change the diaphragm stiffness significantly and consequently change the primary mode of action of such buildings from bending to shear.

In this chapter, analytical results, including both the linear-elastic and the nonlinear-inelastic behavior, are presented for the three component test specimens and the model assemblage test structure. This analytical study is conducted by using the computer program IDARC (15), developed by the investigators at SUNY/Buffalo. The IDARC program is specially developed for the analysis of reinforced concrete structures with floor diaphragms and has the capability of analysing three-dimensional structure systems under static and dynamic loadings in both the linear-elastic and the nonlinear-inelastic ranges. Using a micro-model approach, the amount of the program input

data is minimized.

The following analyses were conducted mainly in order to predict the overall behavior of the specimens:

- Two dimensional analysis of the three model component specimens (shear wall, frame and slab).
- Three dimensional analysis of the model assemblage test structure.

The nonlinear-inelastic analytical results of the model assemblage test structure was closely examined by the investigators at both Lehigh University and SUNY/Buffalo. The design of the model assemblage structure was modified several times in order to achieve the desired dynamic inelastic behavior in the shaking table test. The analytical results were also used in the planning of instrumentation, test setups and prediction of the damage development for the quasi-static cyclic loading tests on the component specimens and the model assemblage.

3.1.1 IDARC Program

The IDARC program package consists of three parts:

1. Static Response Analysis

The main program performs a static analysis to determine component properties such as yield moment strength, cracking moment, and the corresponding curvatures as well as the ultimate failure mode of the structure.

2. Dynamic Response Analysis

A second part performs a step-by-step inelastic analysis. The dynamic response analysis can be performed by the program under both horizontal and vertical base excitations. The hysteretic behavior of the constituent components is included in establishing the overall response of the structure. A major part of the dynamic analysis involves the determination of

independent response of selected substructures.

3. Applications: Substructural Analysis and Damage Analysis

This part consists of the analysis of selected substructures and a comprehensive damage analysis.

Depending on the number of output histories requested, the program can create several output files in addition to the main output file. The output files allow the user to conduct post-processing of analytical results.

In the IDARC program, five types of elements are used for modelling structural components.

1. Beam elements

Beams are modelled as continuous flexural springs. Shear deformation is coupled with flexural effects by means of an equivalent spring which is assumed to act in series with the flexural spring.

2. Column elements

Columns are modelled similarly to beam elements. Axial deformation in the columns is included but its interaction with bending moment is ignored, thus allowing axial effects to be uncoupled.

3. Slab-shear wall elements

Slab and shear wall are modelled as a series combination of flexural and shear-deformation springs.

4. Edge column elements

Edge columns of a shear wall are modelled separately as one-dimensional springs.

5. Transverse beam elements

Transverse beams are modelled as elastic springs with one vertical and one rotational (torsional) degree of freedom.

Empirical equations are used to determine the component properties

of these elements.

3.2 Earthquake Record

The normalized and scaled record of the TAFT, California earthquake of July 21, 1952, is selected as input ground motion for the inelastic dynamic analysis. The scaled acceleration record used in this analysis is shown in Fig. 3-1. The maximum acceleration is limited to 0.959 g due to the capacity limitation of the shaking table at SUNY/Buffalo. In order to conform with the similitude requirements, the time scale is compressed by a factor $1/\sqrt{L_r}$ or 1/2.45.

In comparison with other earthquake accelerograms, the TAFT accelerogram includes a wider range of frequencies. This characteristic of the TAFT accelerogram induces a more pronounced floor diaphragm action of the model structure after the yielding of the slab panels, the condition which is the subject of this experimental study (16).

3.3 Analytical Studies

The three component model structures (shear wall, frame and slab) and the model assemblage structure are analyzed for both the static and the seismic responses. The results of the analyses are presented in this section.

In the static response analyses, the collapse mode analysis is employed to identify the failure mechanisms. For this purpose, the specimens are loaded by lateral static loads in the transverse (main) beam direction from the left side. The lateral static loads are gradually increased until failure. The failure state is defined by a maximum lateral displacement of 2% of the structural height for the frame and the assemblage, 1% of the structural

height for the shear wall, and 0.5% of the panel length for the slab.

3.3.1 Analytical Results of the Three Model Components

The failure sequence, monotonic load behavior and dynamic load behavior are presented in detail for each component model structure as follows.

Shear Wall: In the static analysis, the bottoms of both shear walls yield simultaneously at a lateral load of 10.59 kips, with a bending moment of 173.73 kip-in. in each wall. At a lateral load of 11.06 kips, a plastic hinge forms in the coupling beam at the left end, with a bending moment of 11.55 kip-in.. When the lateral load reaches 11.24 kips, a second plastic hinge forms at the right end of the beam with a bending moment of 10.70 kip-in. At this stage, the top displacement of the shear wall is 0.37% of its height (0.133 in.). But, the structure still can take additional lateral load on account of strain hardening of the reinforcement. Failure state as defined above is reached, when the top lateral displacement reaches 1% of the height of the wall (0.36 in.). The corresponding lateral load is 11.32 kips. The ultimate lateral displacement was 1.89% of the height of the wall (0.68 in.), at an ultimate lateral load of 11.75 kips, at which structural unloading starts.

The monotonic behavior of the shear wall under lateral load is plotted in Fig. 3-2. The plot shows that yielding of the bottoms of the wall reduces the structural stiffness by 98%. After this point, the lateral load only increased by 9.2% to the final failure stage. The figure also shows the shear wall component to be highly ductile, a favorable condition for seismic resisting structure systems.

To illustrate the dynamic inelastic behavior of the shear wall, several time histories of the structure have been plotted. Fig. 3-3 shows the top displacement and the base shear force histories. The time duration is 4.62

seconds. The maximum base shear is 8.58 kips, 73% of the static lateral load resistance. The history of base shear force vs. the top displacement is presented in Fig. 3-4 and the history of the curvature vs. bending moment in Fig. 3-5 for the bottom of the shear wall. Fig. 3-4 shows very little strength deterioration and stiffness degradation. The plot of the curvature vs. bottom bending moment history exhibits the local dynamic inelastic behavior at the bottom of the shear wall, the non-linear behavior of which was mainly due to in-plane bending. Table 3-1 gives the yielding sequence of the shear wall.

Frame: The frame analysis shows that yielding occurs first in the beam, after which the frame stiffness is reduced by 74%. The yielding takes place at a lateral load of 0.25 kips, a beam bending moment of 6.87 kip-in, and a lateral top displacement of 0.06% (0.023 in.) of the height of the frame. As the load increased, the bottom of one column plastified at a bending moment of 8.16 kip-in.. At this stage, the lateral load has increased by 87% from initial yield, to 0.47 kips, and the top displacement has increased by 344%, to 0.28% (0.1 in.) of the height of the frame. At a lateral load of 0.58 kips, the bottom of the other column yields with the same bending moment. The top displacement at this stage is 0.6% (0.22 in.) of the height of the frame. With three sections plastified, the frame stiffness reduces to only 3% of its initial elastic value and the load-deflection curve is almost flat. The failure state is reached when the lateral displacement reaches 2.0% (0.72 in.) of the height of the frame. The ultimate lateral load is 0.6 kips. The static monotonic behavior of the frame is shown in Fig. 3-6. The stiffness degradation can be seen clearly in this plot.

Inelastic dynamic responses of the frame are shown in Figs. 3-7 and 3-8. Fig. 3-7 gives the histories of the top displacement and the base shear of the frame under the excitation of the TAFT earthquake ground motion. The time

duration is 3.4 seconds. In the dynamic responses, the ultimate strength of the frame is only 87% of the static ultimate strength. The maximum top displacement is only 22%. The history of the top displacement vs. the lateral displacement is presented in Fig. 3-8. Table 3-2 gives the yielding sequence of the frame.

Slab: For the static analyses, only the in-plan properties of the slab are considered.

Inelastic behavior is first detected at a transverse section 15 in. away from the center of the supported edge, where several negative longitudinal reinforcing bars are discontinued. The in-plane shear force causing "initial yield" of the slab is 3.65 kips and the corresponding in-plane bending moment at the section is 367.03 kip-in. The in-plane displacement of the slab at this stage is 0.011% (0.005 in.) of the panel length of the slab. This yielding reduces in-plane displacement of 0.50% (0.24 in.) of the slab panel length. The in-plane load at this stage is 4.2 kips and the corresponding in-plane bending moment reached is 435.99 kip-in. At the ultimate stage, the in-plane displacement is 0.9% (0.43 in.) of the slab panel length, the ultimate in-plane load is 4.4 kips and the maximum in-plane bending moment is 439.14 kip-in. This bending moment is 6% higher than the design bending moment of 415 kip-in.. The monotonic behavior of the slab is shown in Fig. 3-9.

Fig. 3-10 gives the in-plane displacement and shear force time histories. In the dynamic responses, the slab reaches a maximum displacement of 0.24 in. and an in-plane shear force of 6.48 kips. The time duration is 4.8 seconds. The time history of the in-plane displacement vs. the shear force is plotted in Fig. 3-11. The diagram exhibits unsymmetrical behavior of the slab. The displacement in one direction is 26% larger than that in the opposite

direction. The time history of the curvature vs. in-plane bending moment of the slab is plotted in Fig. 3-12. The plotting shows the local behavior of the slab in in-plane bending.

3.3.2 Model Assemblage

3.3.2.1 Discretization of the Model Assemblage

The model assemblage structure is analysed in three dimensions. The overall dimensions of the model structure are shown in Fig. 2-1 and the discretization of it in Fig. 3-13. The two interior slab panels are further divided into three regions in the longitudinal direction indicated by S2, S3, S4, S5, S6, and S7. The reason for this subdivision is to reflect the change of the slab reinforcement in the longitudinal direction (between positive and negative moment regions). The subdivision also provides a better lumped mass distribution and a more accurate representation of the yield penetration along the interior slab panels.

3.3.2.2 The Collapse Mechanism Under Monotonic Lateral load

Under monotonically increasing static lateral loads, the collapse mode analysis performed by the IDARC program is used to identify the failure mechanism for the model assemblage structure. For this purpose the model structure is loaded in the transverse direction at the floor slab level, the load being distributed along the longitudinal dimension. The gravity load due to self weight is applied along the transverse beams. The yielding sequence of the model structure members is observed as the lateral load increases. The failure state is defined as that when the maximum lateral displacement reaches 2% of the model structure height.

At the beginning of the analytical study, the design of the assemblage contained the minimum amount of reinforcement required. The collapse mode analysis shows that in this structure, yielding occurs in the shear walls

(the end frames) first, followed by the yielding of the transverse beams and columns of the interior frames. All slab panels remain elastic throughout. Since the main objective of this research is to investigate the effect of the inelastic behavior of the slabs on the distribution of the lateral loads among the lateral load resistance systems, the minimum reinforcement model clearly is not satisfactory. Modifications to the structural design must be made to force the slab panels into inelastic action. This is achieved by changing the amount and distribution of the shear wall vertical reinforcement, and increasing the amount of steel in the coupling beams (B1and B5), thus increasing the yielding strength of the shear walls. The wall vertical reinforcement was increased from 0.46% to 0.85% of the gross wall area. Most of the vertical steel (60%) are placed at the wall edges, effectively forming strong boundary columns. This change increased the in-plane bending strength of the shear wall by 75% and allowed for the yielding of the interior slabs to occur prior to the yielding of the shear walls.

Table 3-3 displays the yielding sequence of the modified model structure. The slab panels yield at a lateral load of 17.26 kips. However, the shear walls remain elastic. Eventually the structure fails at an ultimate lateral load of 21.46 kips.

3.3.2.3 Seismic Responses of the Model Assemblage

The main goal of the experimental study is to test the model assemblage structure with inelastic floor diaphragms under simulated earthquake motion as well as static cyclic lateral load. While the static load test presents no limitation to the model structure, the test on the shaking table requires careful consideration in view of the limited capacity of the shaking table. The key parameter here is the amount of live load to be attached on the model structure in order for the table to shake the structure

into the inelastic range with yielding of the slab during the test. For this purpose, a parametric study was conducted by the researchers at SUNY/Buffalo. From this study, it was decided 50% of the service live load (80 psf) would be used on the model assemblage structure for the shaking table test. The optimal arrangement of the combination of this live load with the additional self-weight is shown in Fig. 2-5. Significant inelastic behavior of the slab is expected under the excitation by the Taft earthquake record. This same arrangement will be used for both the static tests at Lehigh university and the dynamic tests at SUNY/Buffalo.

The analytical response of the model assemblage structure under 50% live load and the scaled Taft earthquake motion, with the maximum acceleration of 0.95 g (see Fig. 3-1) is presented in the following paragraphs.

The time history plots of the displacement, base shear and the corresponding hysteresis curves for the middle and the end frames are given in Figs. 3-14 and 3-15. It is noted that the middle frame peak displacement is about five times that of the end frame, which indicates that the inelastic flexibility of the slab panels plays an important role in the dynamic inelastic response of the model assemblage structure.

To illustrate the inelastic behavior of the floor slab system, the horizontal slab drift (the relative displacement between the middle frame and the shear wall) and the end slab panel in-plane shear history are shown in Fig. 3-16. The non-linear behavior of the slab interior panels is demonstrated by the slab moment-curvature plots, as shown in Fig. 3-17.

Table

Table 3-1: Yielding Sequence of Shear Wall

YIELDING SEQUENCE	LINKING BEAM M		SHEAR WALL M AT BOTTOM		LATERAL LOAD	DISPLACEMENT
	Left	Right	Left	Right	kips	%H
Wall Btm.	8.56	-6.46	173.73	173.73	10.59	0.043
Beam,Left	11.55	-9.64	176.45	176.45	11.06	0.163
Beam,Right	11.81	-10.7	178.21	178.49	11.24	0.369
Failure	11.86	-10.75	179.42	179.70	11.32	1.00
Ultimate	11.88	-10.77	179.54	179.83	11.57	1.8

M = moment, kip-in

Table 3-2: Yielding Sequence of Frame

YIELDING SEQUENCE	BEAM M		COLUMN L. M		COLUMN R. M		LATERAL LOAD	DISPL.
	Left	Right	Top	Bottom	Top	Bottom	kips	%H
Beam,Right	-2.90	-6.87	2.53	-0.15	4.67	-6.05	0.25	0.06
Column,R. Bottom	-2.83	-6.91	2.84	4.04	-5.72	8.16	0.47	0.28
Column,L. Bottom	-2.73	-6.96	3.27	8.16	-5.77	8.18	0.58	0.60
Failure & Ultimate	-2.55	-7.17	3.10	8.26	-5.88	8.25	0.60	2.00

M = moment, kip-in

Table 3-3: Yielding Sequence of Assemblage Structure

END FRAME MEMBER REINFORCEMENT AREA (in^2)		BASE SHEAR (kips)	MEMBER YIELDING
WALL	BEAM		
0.336	At=0.08	12.72	B3 (Right)
60% at boundaries	Ab=0.08	17.26	S3 (Right), S6 (Left)
		17.51	B2, B4 (Right)
		18.25	C5 (Bottom)
		18.59	C4, C6 (Bottom)
		19.28	C2 (Bottom)
		19.56	C1, C3 (Bottom)
		21.46	S3 (Left), S6 (Right)
		21.46	Structure Failure

Figure

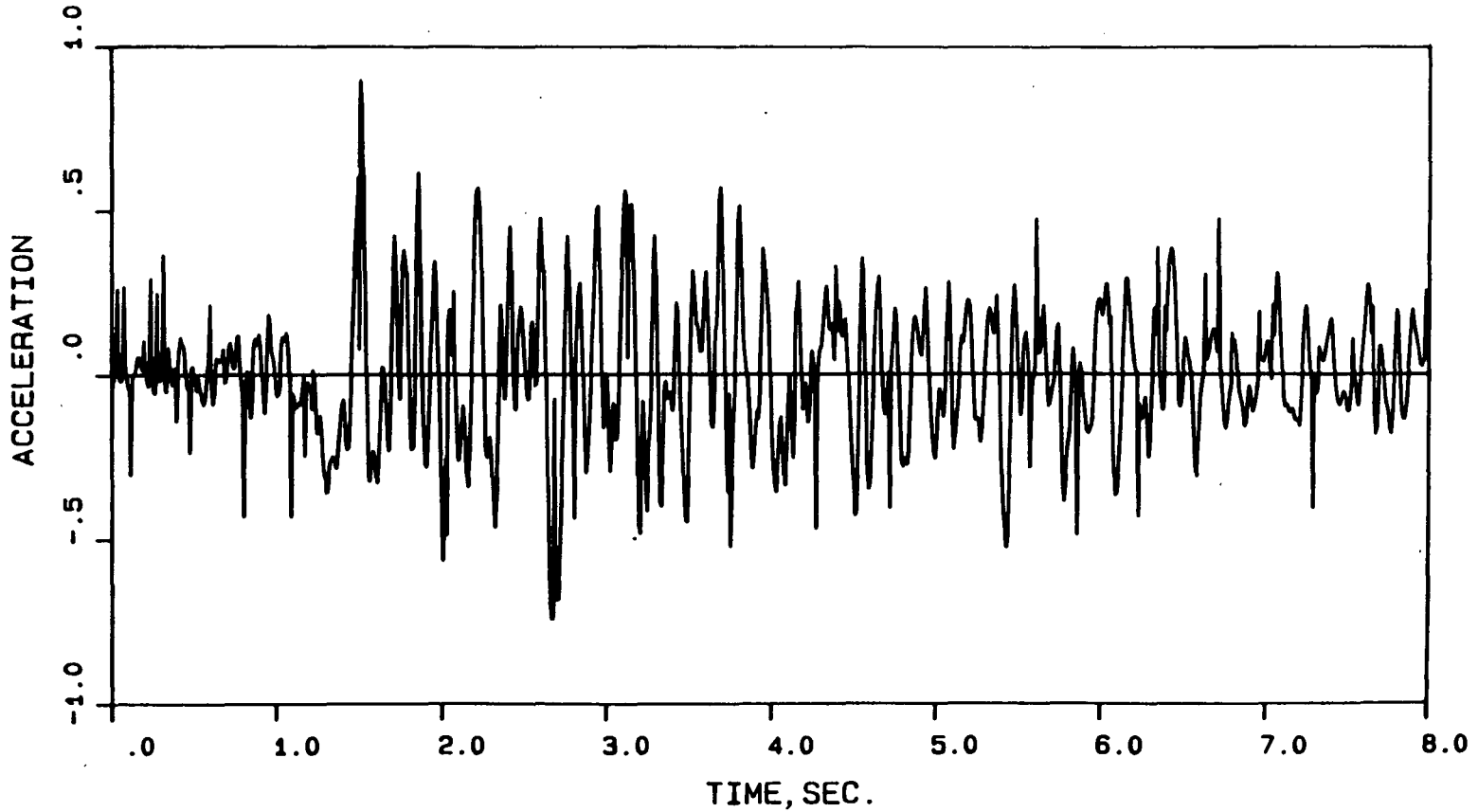

Figure 3-1: Scaled TAFT Earthquake, California, July 21, 1952

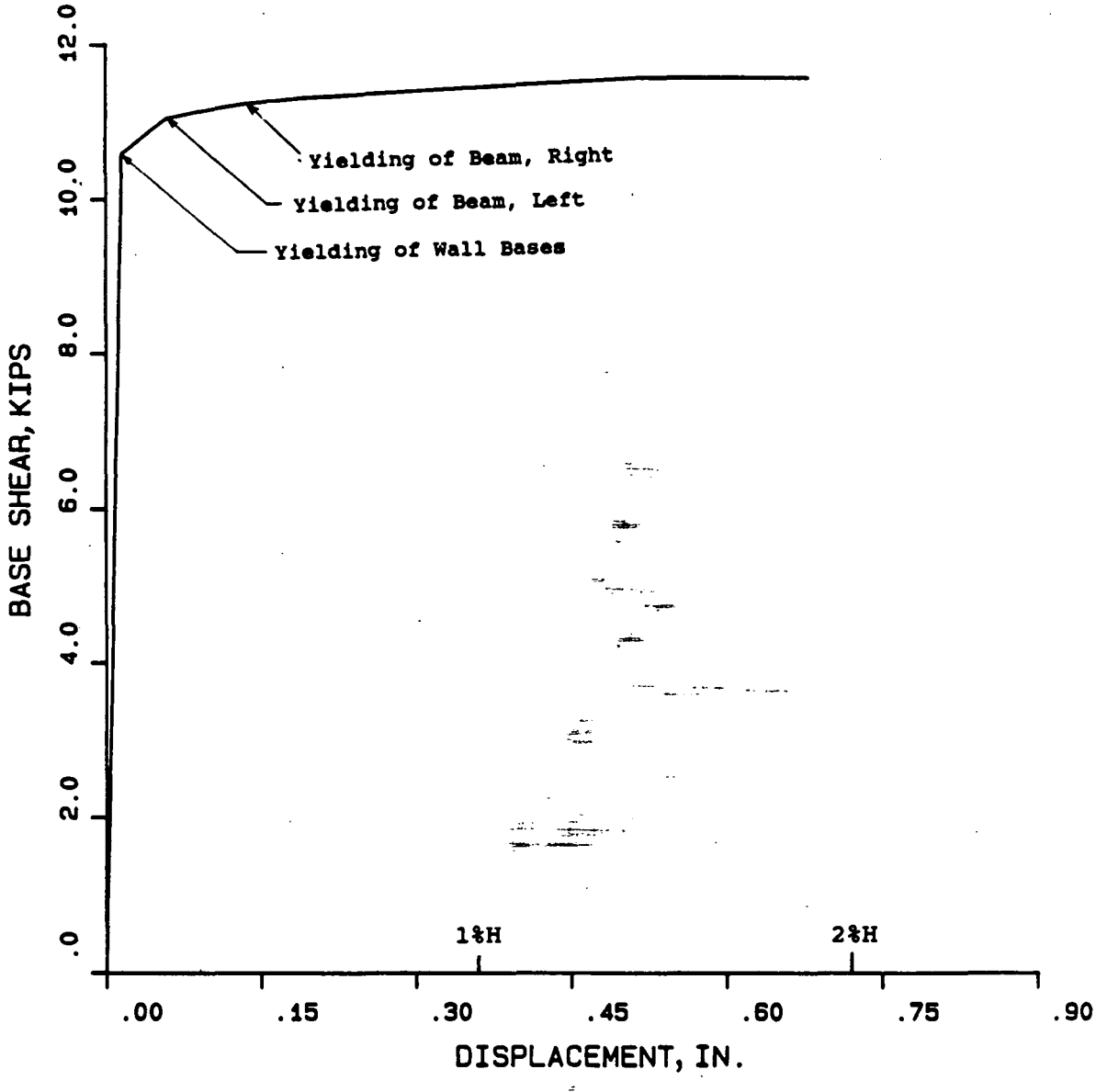

Figure 3-2: Monotonic Behavior of Shear Wall

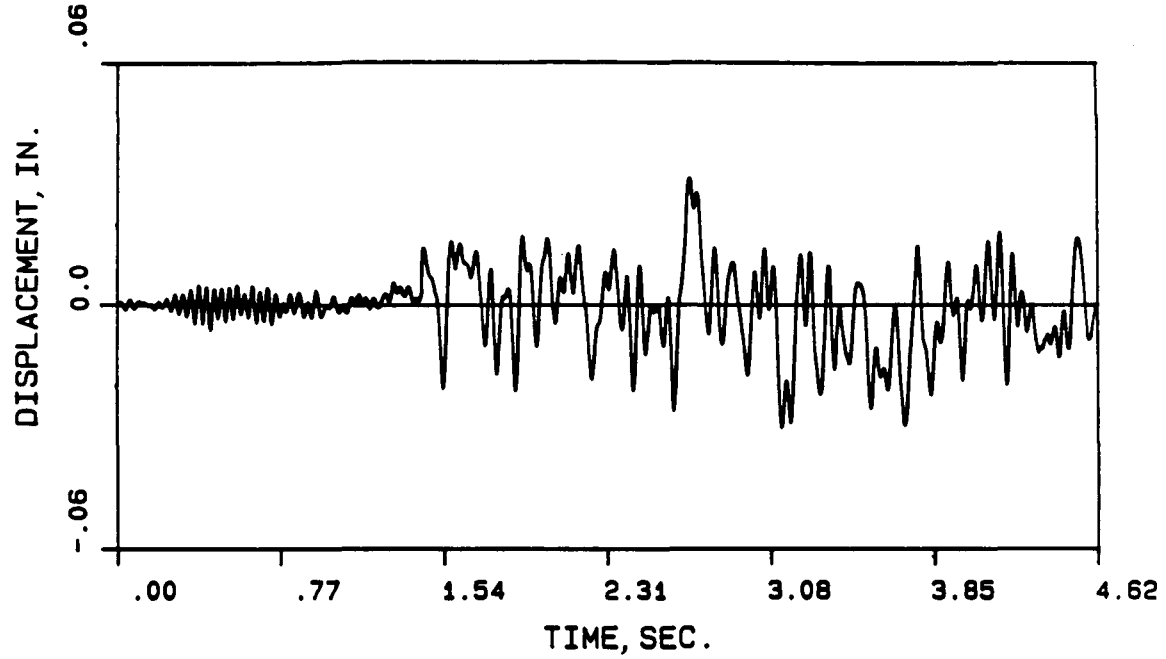

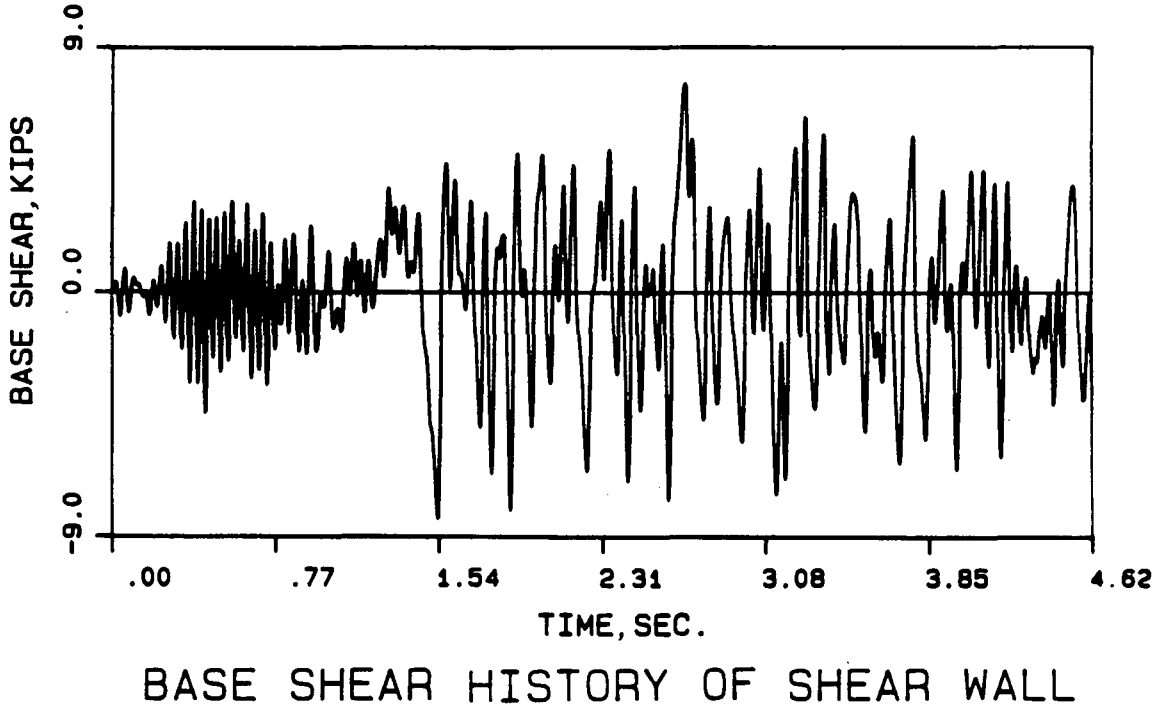

Figure 3-3: Calculated Seismic Responses of Shear Wall

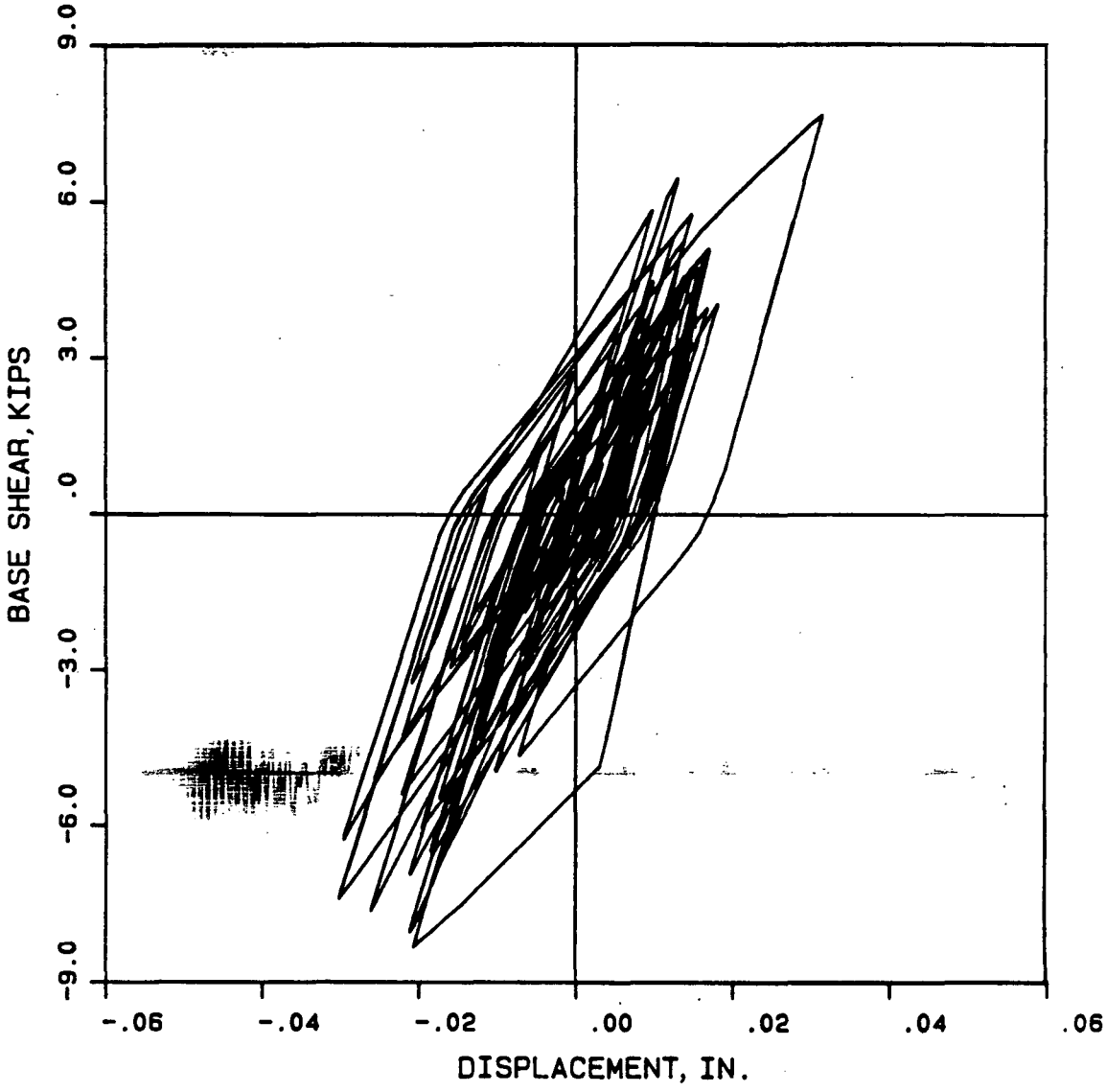

Figure 3-4: Base Shear vs. Displacement Relationships of Shear Wall

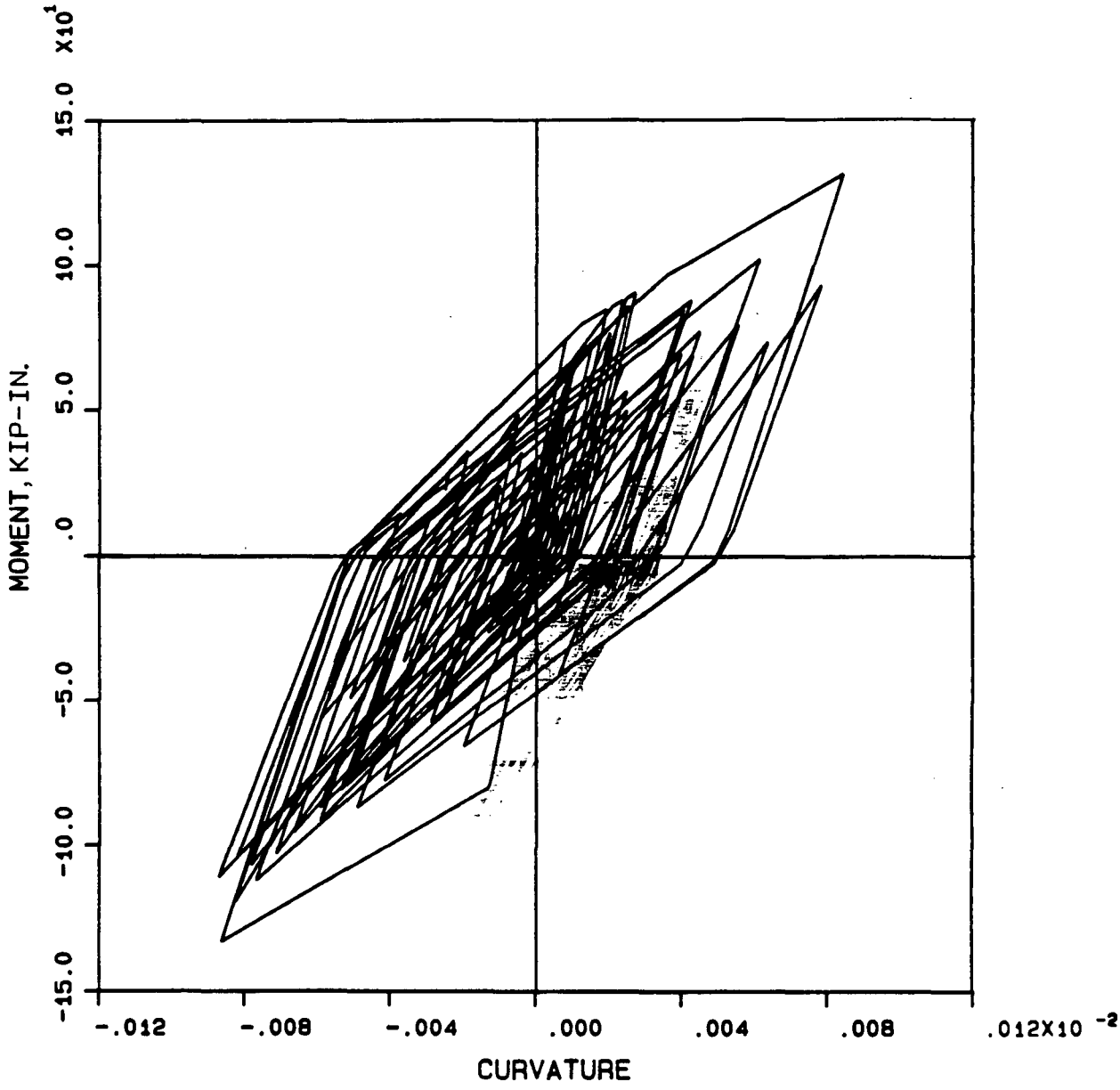

Figure 3-5: Curvature vs. Moment Relationships at Bottom of Shear Wall

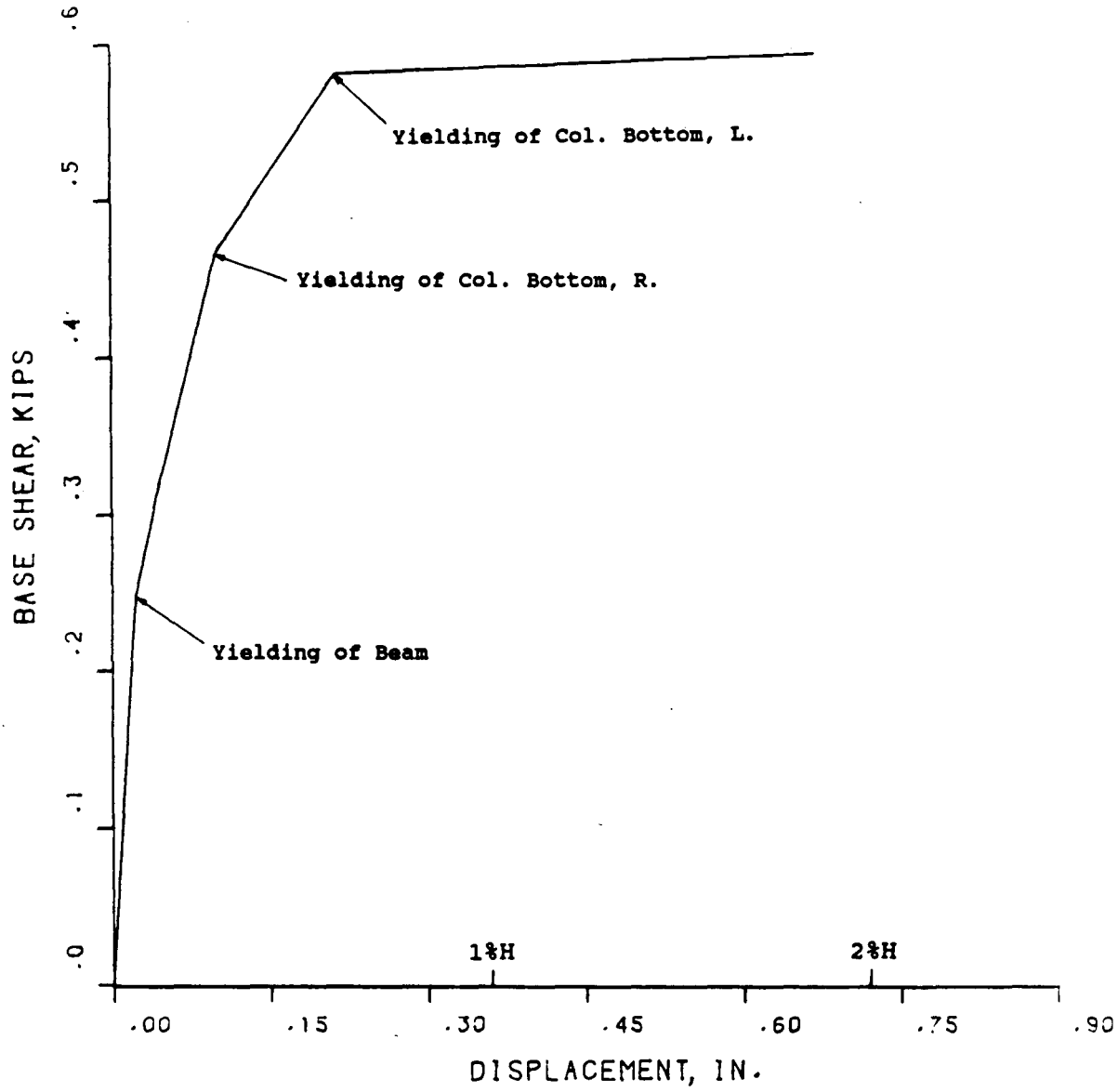

Figure 3-6: Monotonic Behavior of Frame

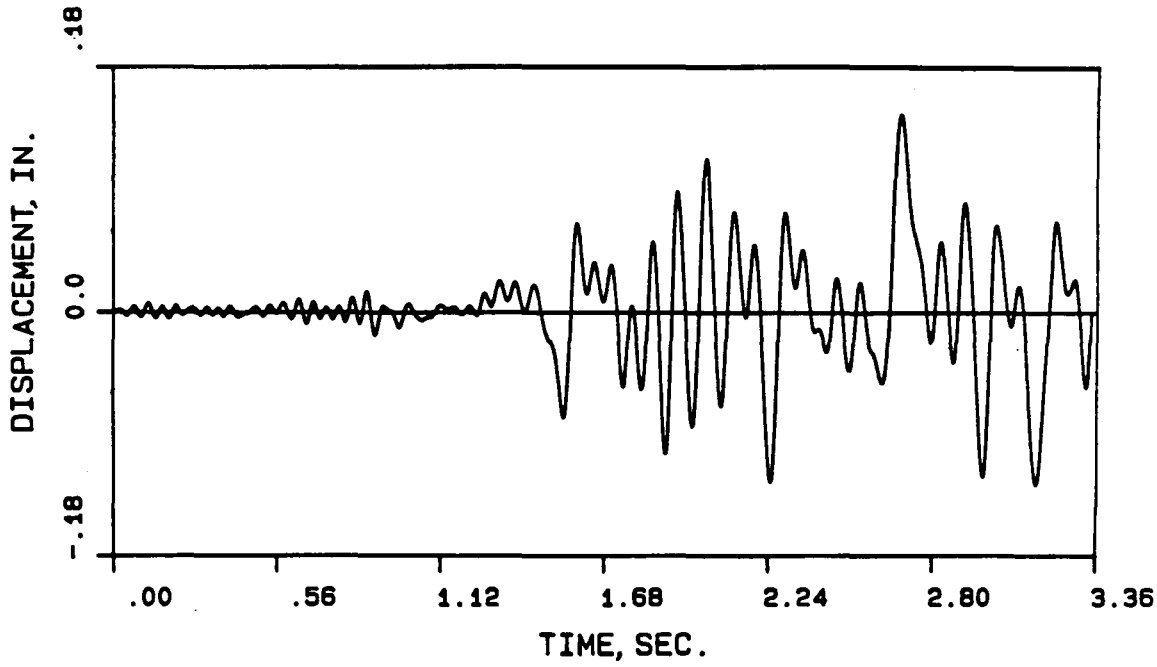

TOP DISPLACEMENT HISTORY OF MIDDLE FRAME

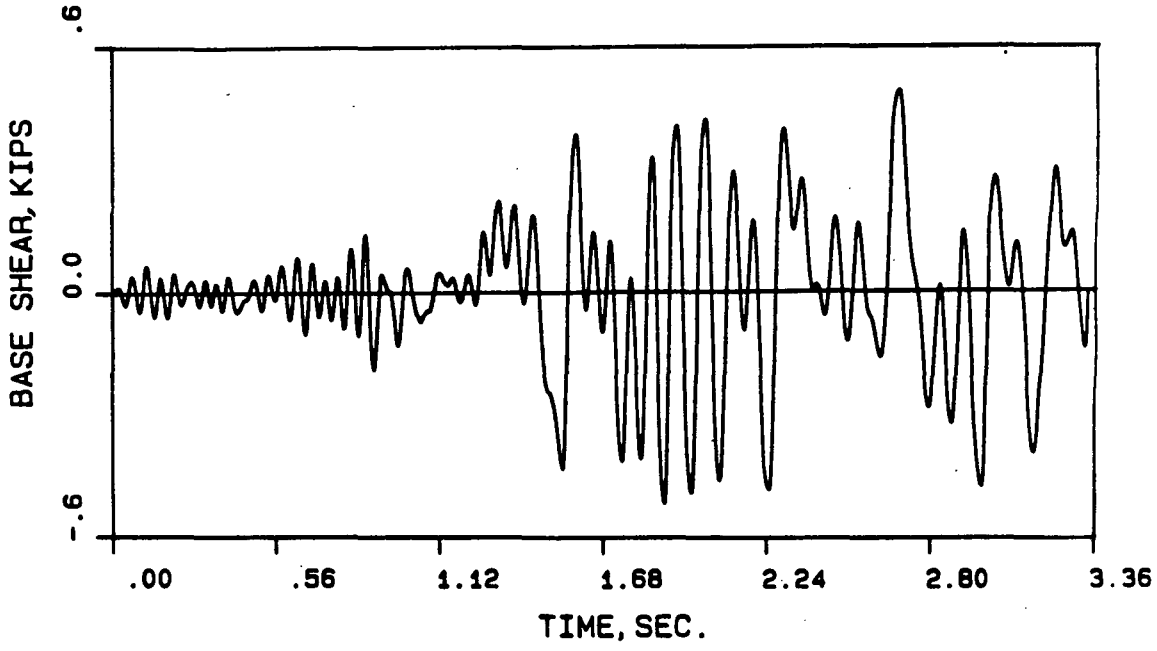

BASE SHEAR HISTORY OF MIDDLE FRAME

Figure 3-7: Calculated Seismic Responses of Frame

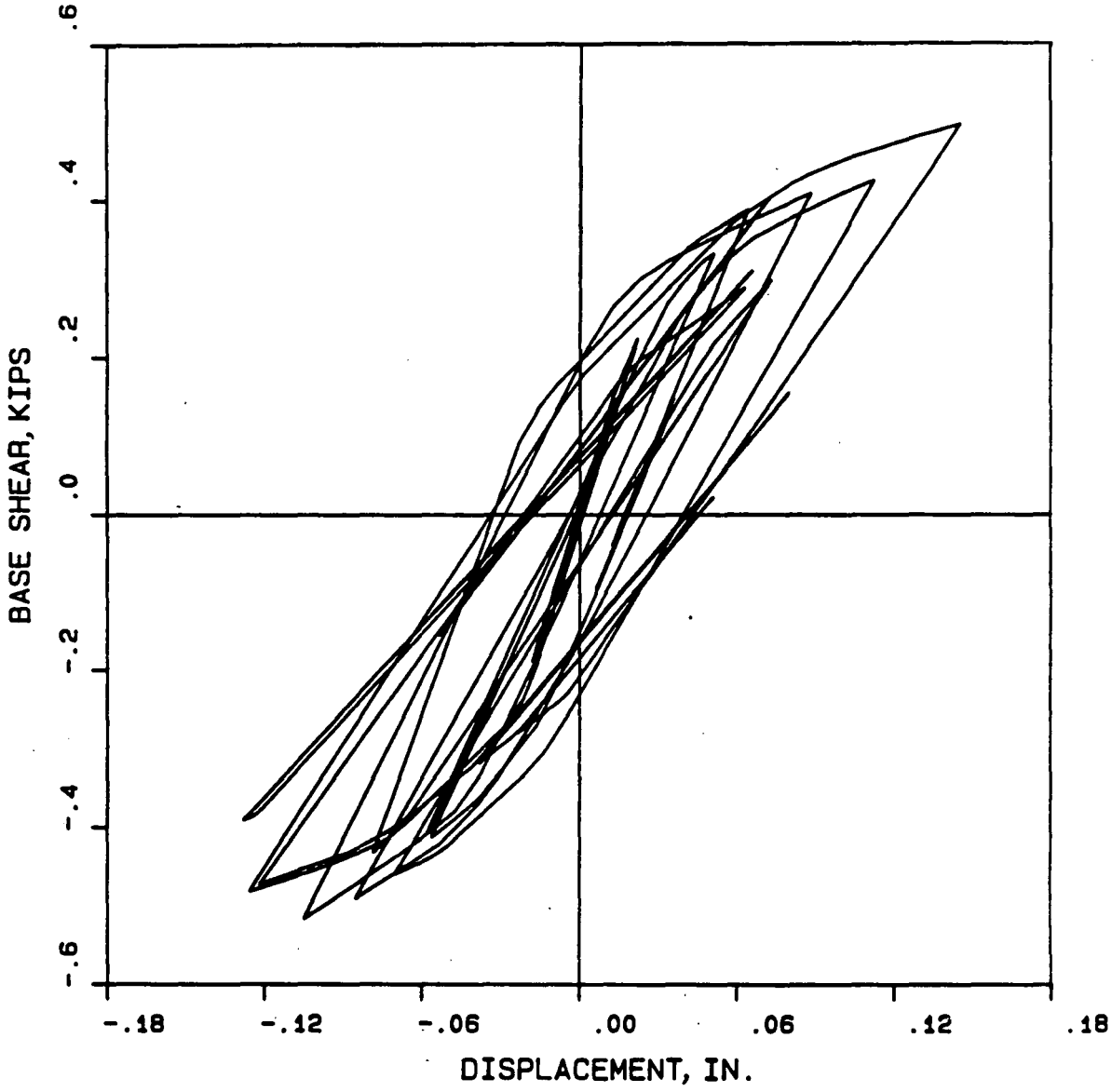

Figure 3-8: Base Shear vs. Displacement Relationships of Frame

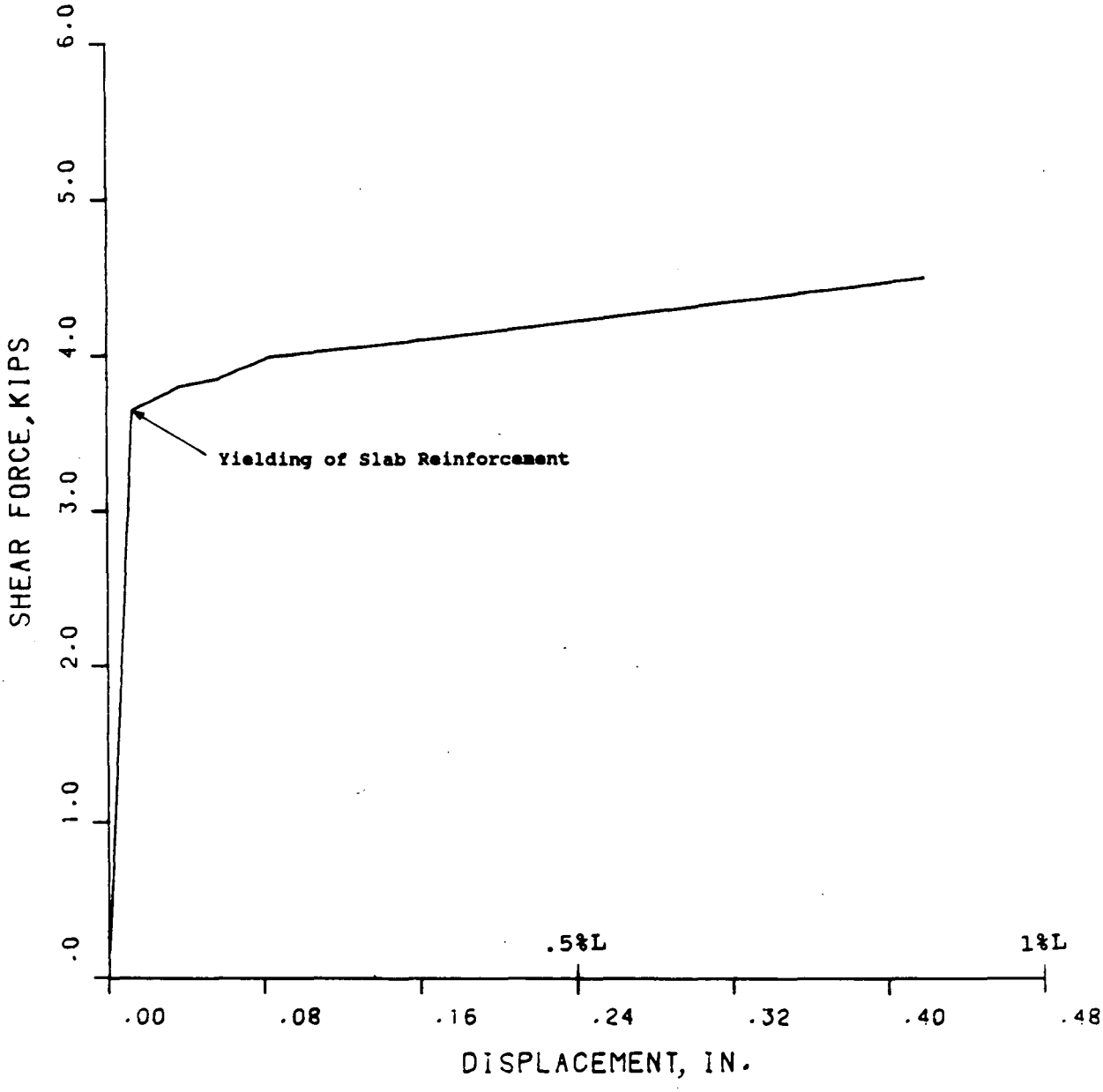

Figure 3-9: Monotonic Behavior of Slab

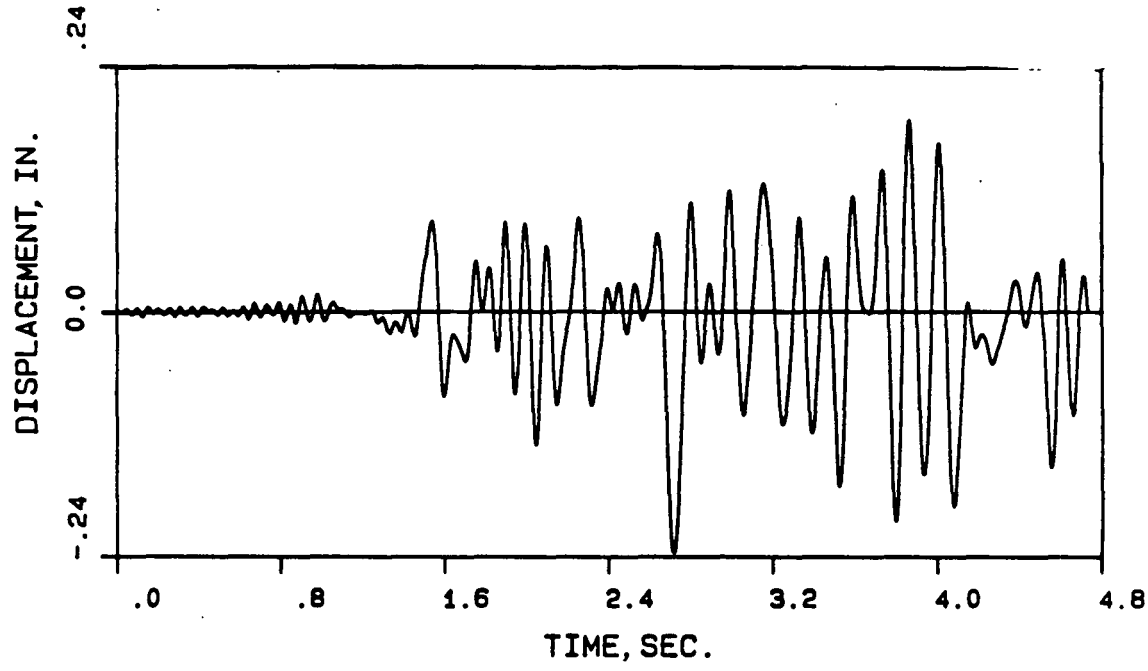

DISPLACEMENT HISTORY OF MIDDLE SLAB

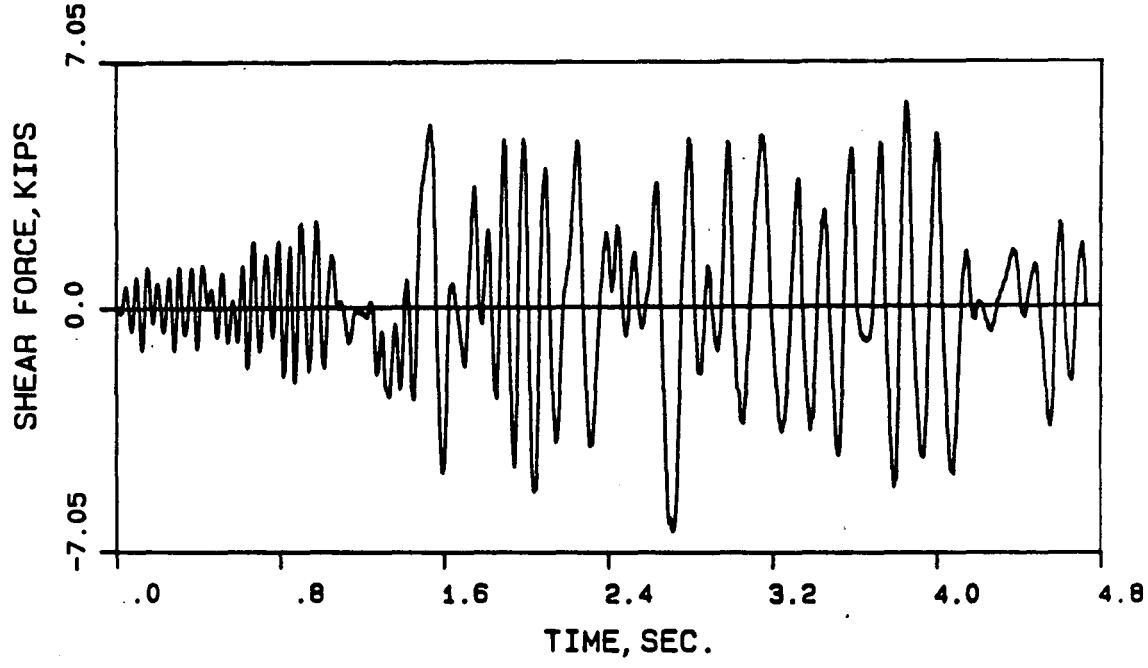

SHEAR FORCE HISTORY OF MIDDLE SLAB

Figure 3-10: Calculated Seismic Responses of Slab

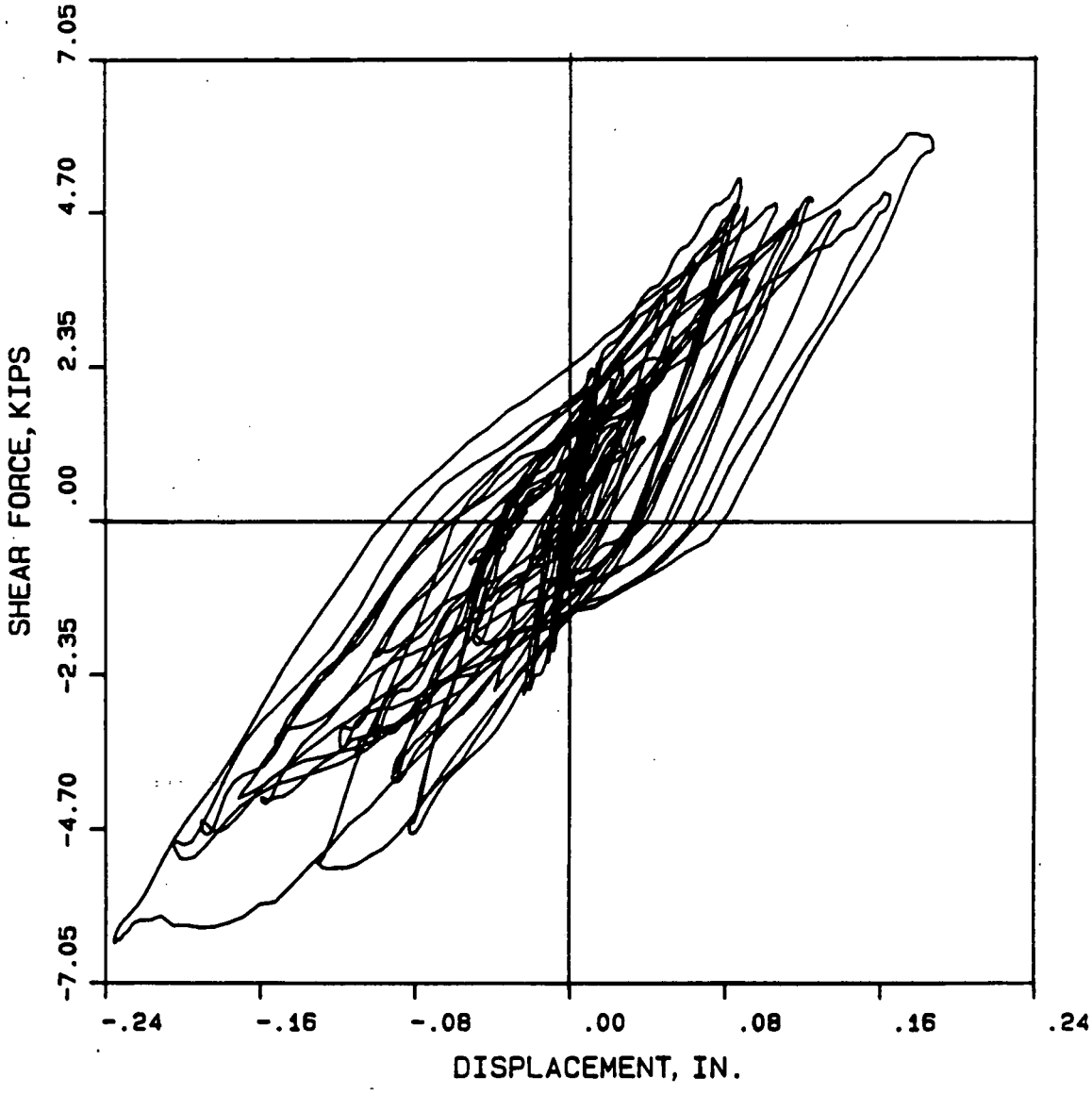

Figure 3-11: In-plane Shear Force vs. In-plane Displacement Relationships of Slab

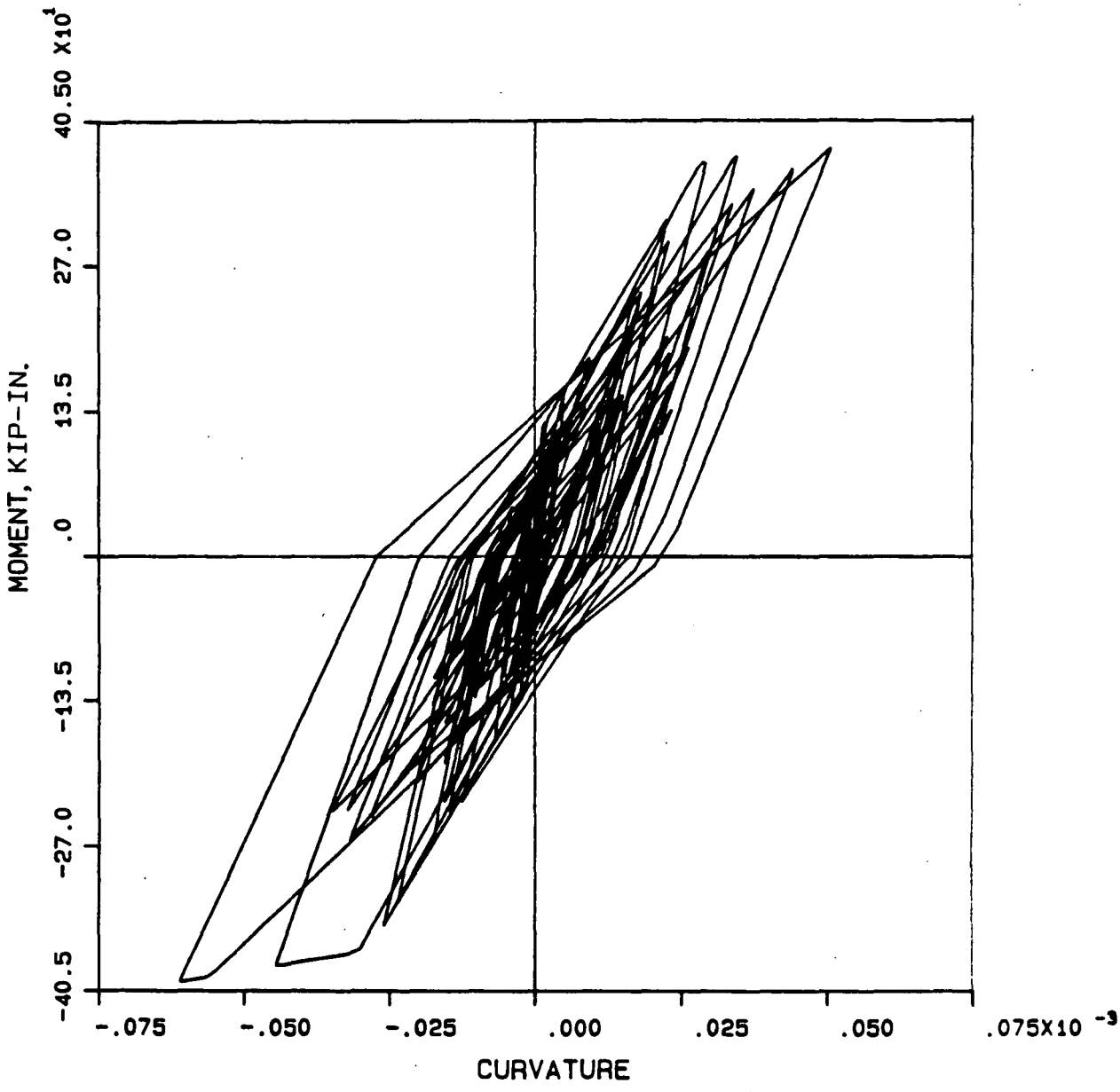

Figure 3-12: In-plane Curvature vs. Moment Relationships of Slab

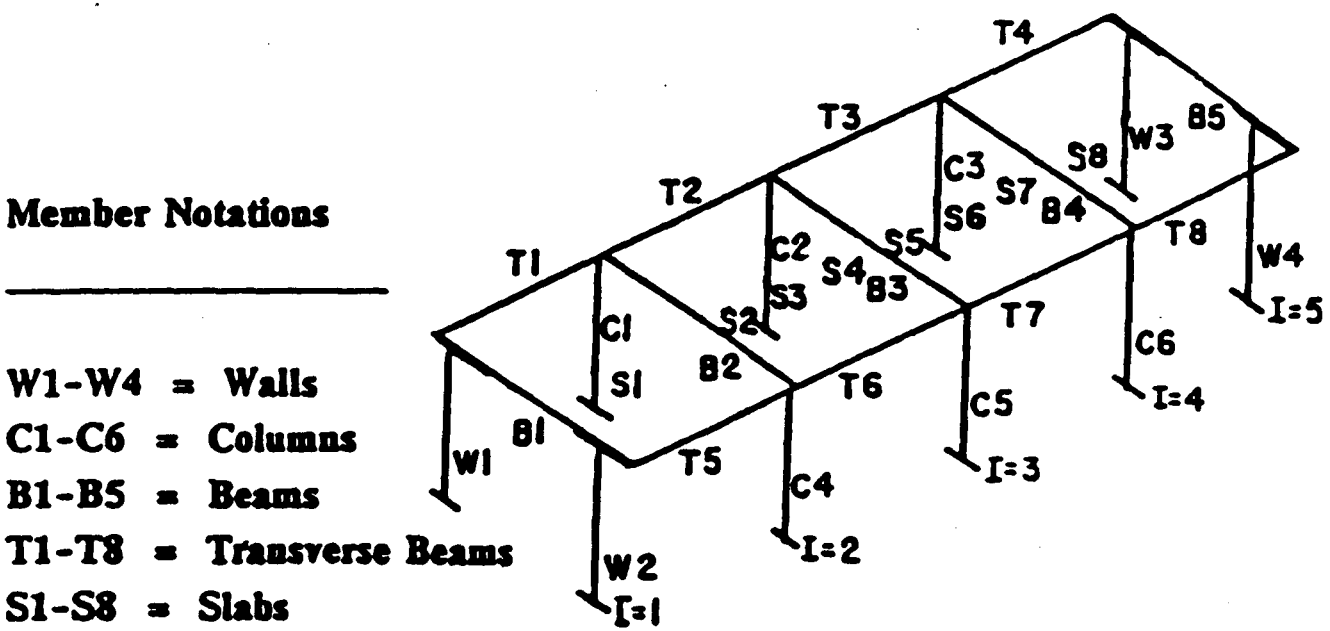

Figure 3-13: Discretization of Assemblage Structure

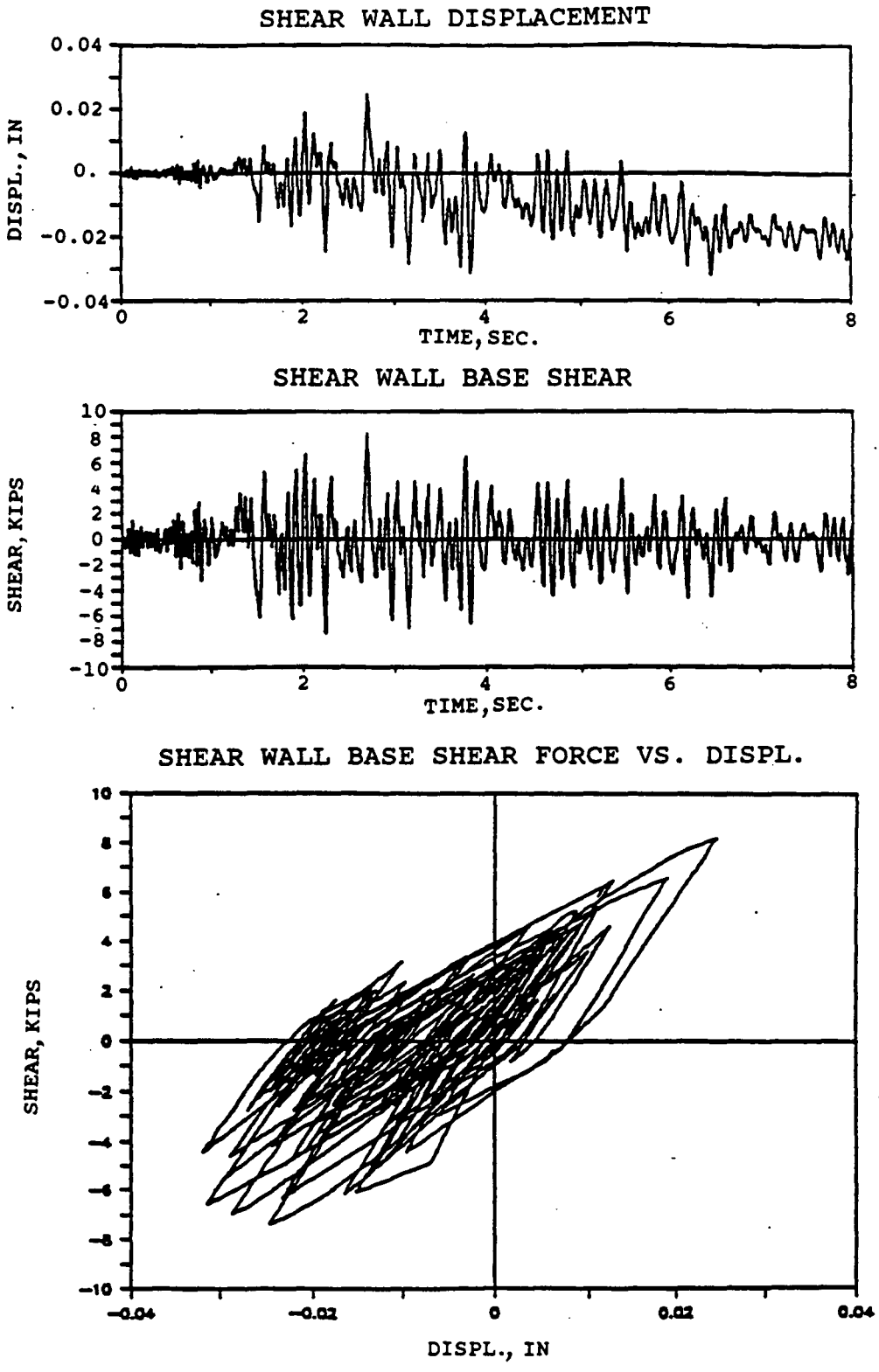

Figure 3-14: Displacement vs. Base Shear Force Relationships of Shear Wall for Assemblage Structure

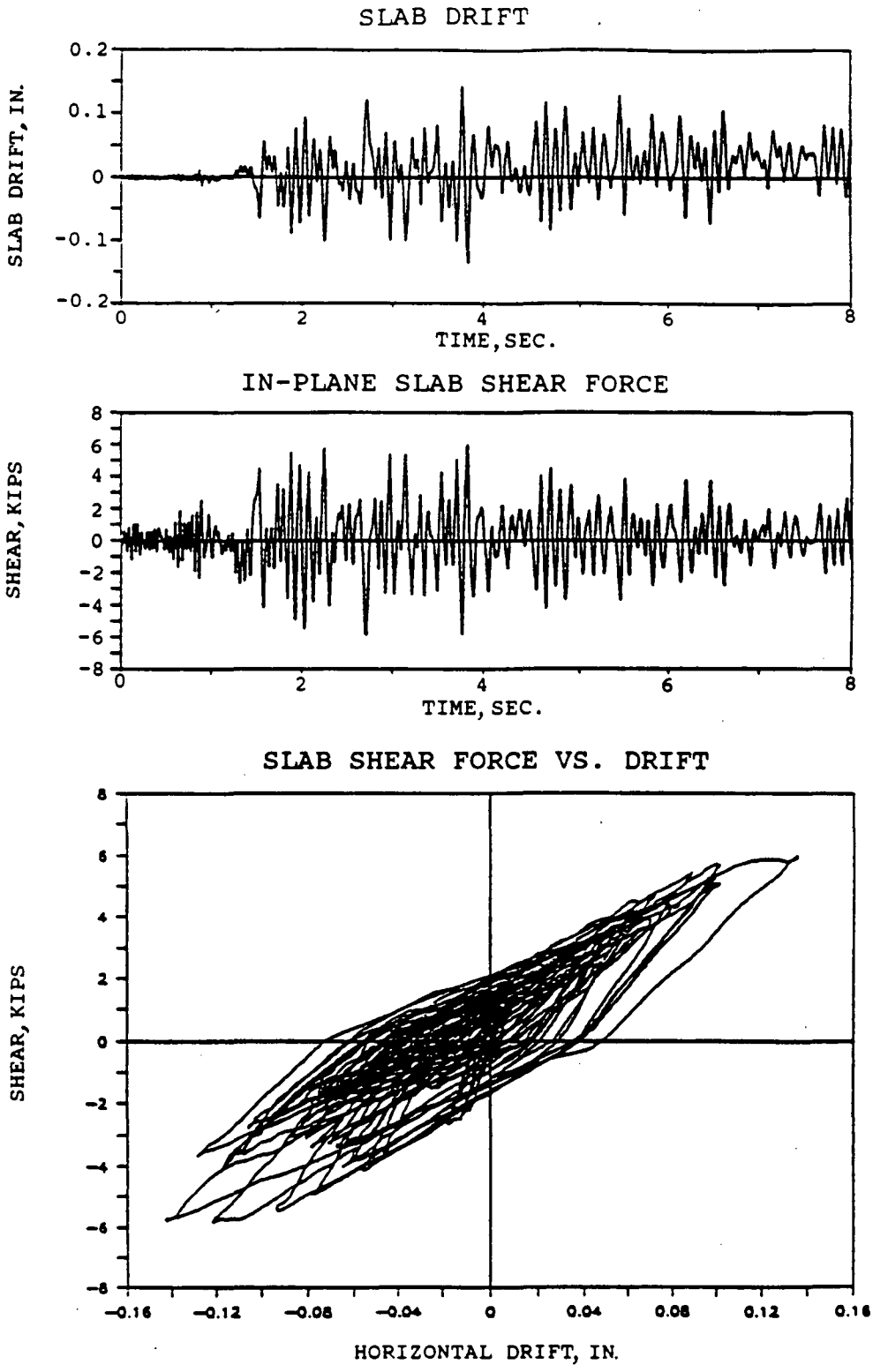

Figure 3-16: Slab Drift (Relative Displ. Between Middle Frame and Shear Wall) vs. In-plane Slab Shear Force Relationships at the End Panel for Assemblage Structure

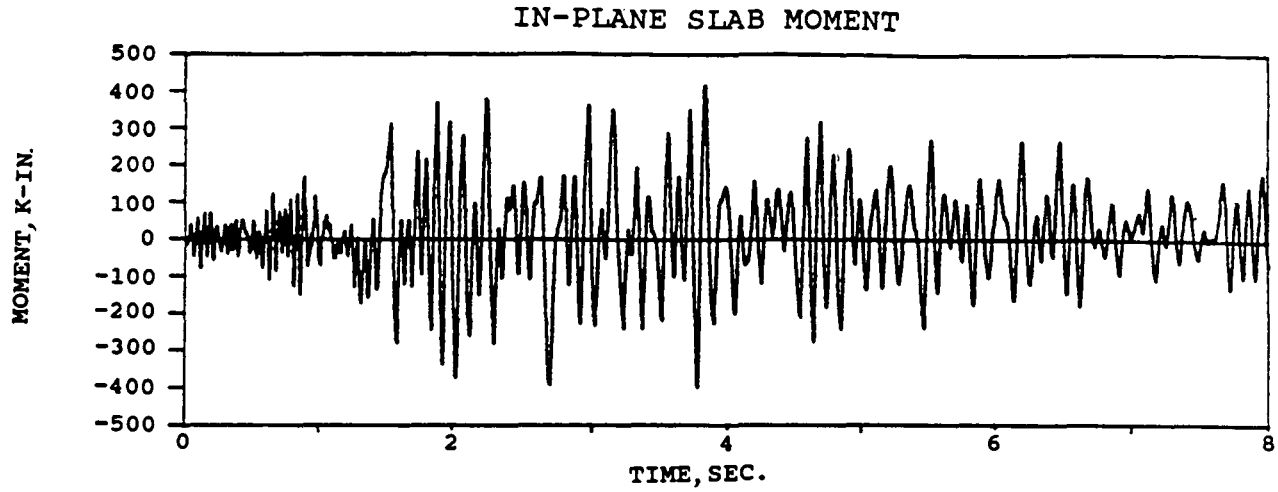

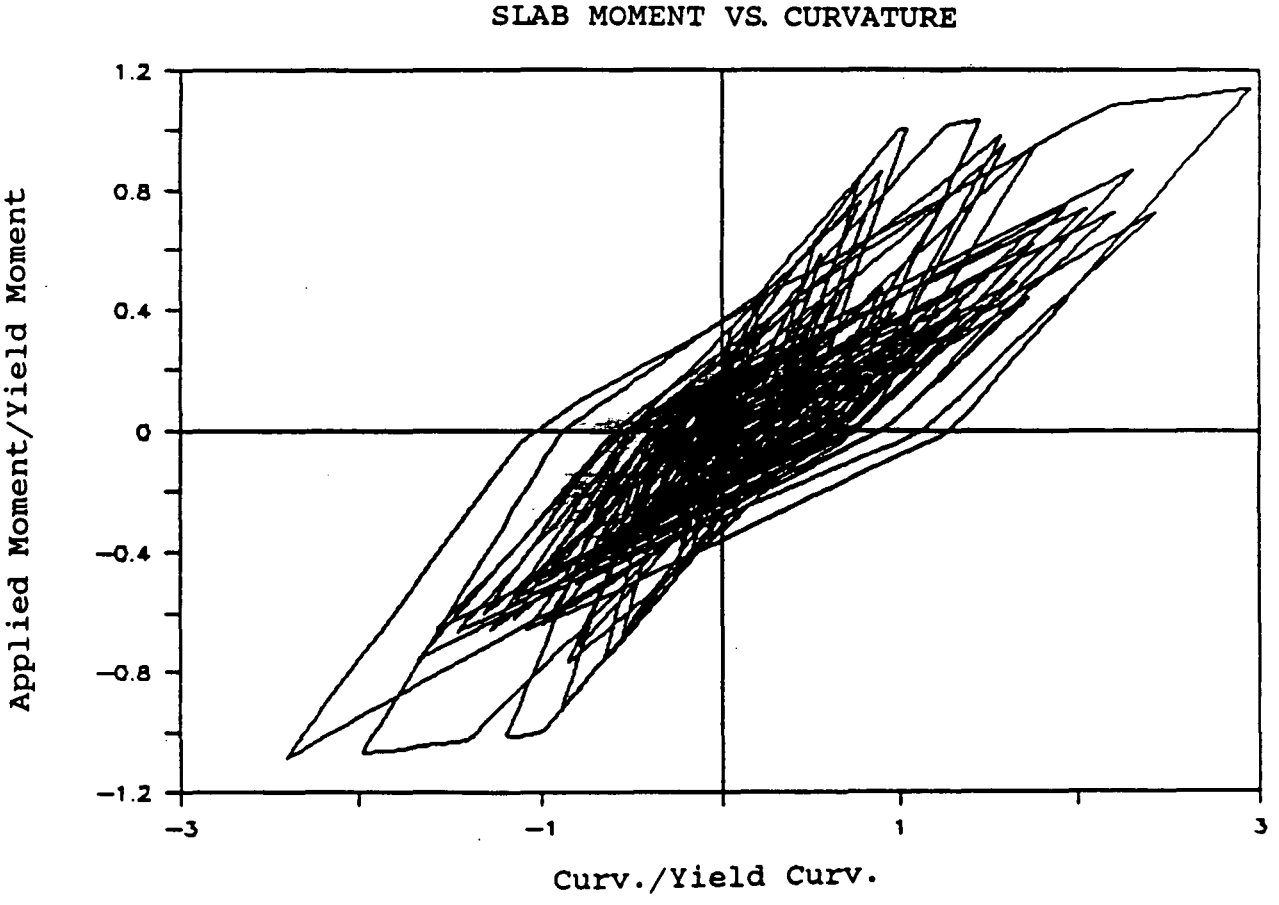

Figure 3-17: Curvature vs. Moment Relationships of the Middle Panel for the Assemblage Structure

Chapter 4
Experiment Planning

4.1 Model Materials

4.1.1 Concrete

The concrete mixture for the model structure was originally designed by the researchers at SUNY/Buffalo, using a naturally graded river sand aggregate,identified as Erie aggregate. The aggregate grading is shown in Table 4-1. The moisture content of the aggregate is 4.7% as delivered. The concrete mix chosen consists of Type III (high early strength) Portland cement, aggregate and water combined in the proportion of 1.0 : 6.0 : 0.75 by weight. Several trial batches of this mix made at Lehigh failed to achieve either a satisfactory consistency or a good workability. A aggregate grading study of the aggregate revealed that there was not enough fine sand particles in the mix. A fine sand named Jersey sand, of which the grading is also shown in 4-1, is added to the aggregate, in the proportion of fine sand and aggregate of 1:6 by weight. In addition, a super-plasticizer EUCON 37 is added to the mix to increase the workability of fresh concrete, and to ease concrete placing. The dosage of the plasticizer is 1 percent to water by volume. The finally adopted proportion of the mix is 1 part (by weight) of Type III Portland cement, 5.83 parts mixed aggregate, and 0.83 part water plus the plasticizer. A 6 in. slump is obtained without the plasticizer. Adding plasticizer causes the slump to increase to 8-1/2 in..

The average compressive strength given by 3 in. x 6 in. cylinders at an age of 28 days is $f_c' = 3900$ psi. The average ultimate strain measured from these cylinders is 0.0045. One typical stress-strain curve of concrete is shown in Fig. 4-1. The average initial Young's modulus determined from the stress-

strain curves is E_c = 3150 ksi. The average splitting tensile strength, determined on the same size cylinders, is f_{sp} = 400 psi.

Typically, concrete with extra-fine aggregates exhibits a higher tensile strength as a fraction of its compressive strengths (21). This has caused considerable difficulty in the conduct of small scale model studies of concrete structures because the model structure does not crack as readily as the prototype. For the concrete used in this study, the ratio of tensile to compressive strength, f_{sp}/f_c', was 0.103, (alternately, $f_{sp} = 6.4\sqrt{f_c'}$). This ratio is very nearly the same as for ordinary concrete. Consequently, the "size effect" is not expected to be significant in this study. In scaling the concrete mixture to produce micro-concrete, it is also found that the concrete compression strength is very sensitive to the water-cement ratio.

4.1.2 Steel

Considerable effort and time were spent on the acquisition of the required small size reinforcements. It was finally decided to buy unannealed D2 and D1 bars, which had very high yield strengths and also very low ductility. An annealing process was then used to lower the yield strength and to improve the ductility. The annealing work was done at a local commercial laboratory. Unfortunately, significant difficulty was encountered in annealing these small size bars because of the extreme sensitivity of the yield strength and ductility of the bars to the annealing temperature and its duration. The annealing procedure finally adopted after many trials was: heating up to 1120°F, holding this temperature for one-and-one-half hours, then cooling down naturally to normal room temperature. The mechanical characteristics of the annealed bars were determined by basic tension tests. The test was repeated four times for each size of bars in each annealed batch. An electric extensometer with a 2.25 in. gage length was used to

measure the strain. Table 4-2 lists the yield strength and the ultimate strength of the reinforcing bars before and after annealing. The values listed in the table for annealed reinforcing bars represent the average of the results of all tests from all annealing batches. Fig. 4-2 shows typical stress-strain curves of these bars.

The light deformation of the D1 and D2 bars, (Fig. 4-3), are not in proportion to the deformation of standard reinforcing bars. However, in view of the very small bar diameters, the bond between concrete and reinforcement is judged to be adequate for the full development of the bars within the development length specified by ACI 318-83 (1). A few pull-out tests verified this judgment.

Smooth G14 wires with a yield strength of 35 ksi were purchased in annealed condition in 10 lb coils. Deformation on the smooth G14 were produced by rolling the coiled wires through two pairs of grooved rollers. The deformed wires were cut into design lengths immediately after being rolled in order to keep them in straight condition. The rolling process caused a significant increase in yield strength and a loss in ductility. Therefore, the deformed G14 wires were annealed again down to 40 ksi yield strength with a satisfactory ductility. The annealing procedure was the same as used for D1 and D2 bars. A typical stress-strain curve for deformed G14 wire is included in Fig. 4-2. The Deformed G14 wires are used as the reinforcement in slabs and the smooth G14 wires as the stirrup reinforcement for all test structures.

In the annealing study of the deformed small diameter reinforcing bars (D1,D2 and G14), it is found that the yielding strengths of annealed bars is totally controlled by the annealing procedure, and independent of the original yielding strengths. Furthermore, the yielding strength and ductility of

small reinforcing bars are found to be much more sensitive to the annealing temperature than the duration of the annealing procedure.

4.2 Component Tests

4.2.1 Test Setups

The testing of the components will be conducted on the dynamic test bed in the Fritz Engineering Laboratory. Special loading frames and fixtures have been developed for these tests. The test setups for the three model components are shown in Figs. 4-4, 4-5 and 4-6.

The test setups for the shear wall and the frame specimens are similar (Fig. 4-4 and Fig. 4-5). For the application and the control of the lateral load on the specimens, a load cell and a mechanical jack are supported horizontally on a reacting beam. A loading frame is connected to the load cell by a pin, and is placed on two end plates which are epoxy-attached to the specimens. Two half circular steel bars, one on each end plate, are used to ensure that the lateral load on the specimen acts at the center plane of the cross section of beam and slab.

For the shear wall component, the concrete footing block is fastened directly to the test bed by 3-in diameter floor anchors. For the frame specimen, a pair of load cells specially designed by the investigators at SUNY/Buffalo are used in order that reaction forces at the base of each column can be directly measured. The specimen is lifted 9 in. off the floor, (Fig. 4-5), and the floor connection is made through a 2 in. think adapting steel plate.

The test setup for the slab specimen is designed to simulate the loading condition of the middle slab panels in the assemblage structure. The specimen is rigidly supported along one enlarged transverse beam. A

triangular steel frame is attached to the opposite edge, as shown in Fig. 4-6. The length of the loading triangular frame (130 in.) is designed to produce the desired ratio of bending moment to shear force at the critical slab section. This ratio is obtained from the analytical results of the assemblage.

The additional gravity loads for these three model components (refer to Section 2.3.2) will be created by hanging steel blocks underneath the slabs.

In order to obtain more detailed information, the three component specimens will be tested through as many loading cycles as possible within the constraints of the laboratory schedule. The proposed loading programs for these specimens are showed in Figs. 4-7, 4-8 and 4-9. A large number of small initial loading cycles are employed to avoid premature overloading of the specimens. To make the test results more helpful in determining the loading programs (11) for the shake table tests, a few small loading cycles are repeated after the structure has been substantial damaged. The strength and stiffness deterioration are observed from repeating loading cycles with large amplitude.

4.2.2 Instrumentation

Instead of localized stress effects, the experimental study of both the assemblage and component specimens is primarily intended to generate information on the global behavior of the test structures. Therefore, few interior gages are used, and no strain gages are placed on the reinforcing bars. A number of surface gages, including rosettes, are used. Six LVDT's are mounted on each specimen to measure vertical and horizontal displacements (Figs. 4-10, 4-11 and 4-12). Clip gages are used to measure section rotations at beam-column or beam- shear-wall joints (Fig. 4-10 and 4-11). Dial gages are used to monitor the movements of the footing. For the

shear wall and frame specimens, one internal concrete strain gage is cast in the transverse beam to measure the axial force in the beam.

The pair of load cells used in the frame tests are designed to monitor the axial and shearing forces, and the bending moment reactions at the each column.

4.3 Assemblage Test

4.3.1 Test Setups

Since the model assemblage structure is very flexible, any transportation of the structure will pose a serious risk of premature damage. Therefore, it is decided to construct the assemblage structure at its test location. Additional weights will be added to the specimen for the static load test, to reflect the effect of structural weight and live load (Section 2.3). These weights will be applied as vertical loads acting at centers of slab panels. Four vertical loading frames will be used for this purpose, but will be designed to allow the slab to deflect laterally. The cyclically applied static lateral load will be produced by four mechanical jacks, each of which will be attached at the center of a slab panel. The purpose of loading the slab at center is to simulate the effect of the inertial forces generated by seismic excitation. These lateral loads will be gradually incremented to bring the structure first into inelastic behavior and eventually to failure. The loading program for each jack will be determined from the actual loading programs of the three component tests.

For the assemblage structure, the footings of the shear walls and frames will be cast directly onto the test bed. The strength of the footings will be over designed to eliminate any failure in the footings during testing.

4.3.2 Instrumentation

The instrumentation will be the same as for the three component specimens. No strain gages will be placed on the reinforcing bars. In order to obtain the information regarding the global behavior of the assemblage structure, five LVDT's will be used to measure the horizontal displacements of the slab, at the five frame locations. Two LVDT's will be mounted at each end shear wall frame in the longitudinal direction to measure the rotation of the end frame. Dial gages will be used at selected critical points to measure the vertical as well as horizontal movements of those points. Some concrete surface strain gages will be used to monitor the shear force in the slab and the shear walls during test. For the critical sections at which cracking and yielding are expected to occur,clip gages will be employed to detect the opening and closing of these sections. One internal concrete strain gage will be cast in the transverse beam for each frame to measure the axial force in the beam as in the shear wall and frame specimens. The angle changes between the center lines of column and transverse beams will be measured by special clip gages.

Table

Table 4-1: Aggregate Grading

SIEVE SIZE	ERIE AGGREGATE AMOUNT RETAINED (g)	ERIE AGGREGATE PASSING (%)	JERSEY SAND AMOUNT RETAINED (g)	JERSEY SAND PASSING (%)	MIXED AMOUNT RETAINED (g)	MIXED PASSING (%)
#4	107	89.2	0	100	107	90.8
#8	396	49.2	29	97.1	401	56.1
#16	326	16.4	53	91.8	335	27.2
#30	113	4.9	155	76.2	139	15.2
#50	31	1.8	459	30.1	108	5.9
#100	11	0.7	260	3.9	54	1.2
Pan	7		39		14	
total	991		995		1158	

Table 4-2: Yielding and Ultimate Strengthes of D2, D1 and G14

	Unannealed Bars			Annealed Bars			
			Deformed			Deformed	Smooth
	D2	D1	G14	D2	D1	G14	G14
Yield Strength	88	106	50	53	51	42	35
Ultimate Strength	97	123	55	68	59	51	51

Unit: ksi

Note: The strengths given in this table are the average values of all coupon tests for each bar type.

Figure

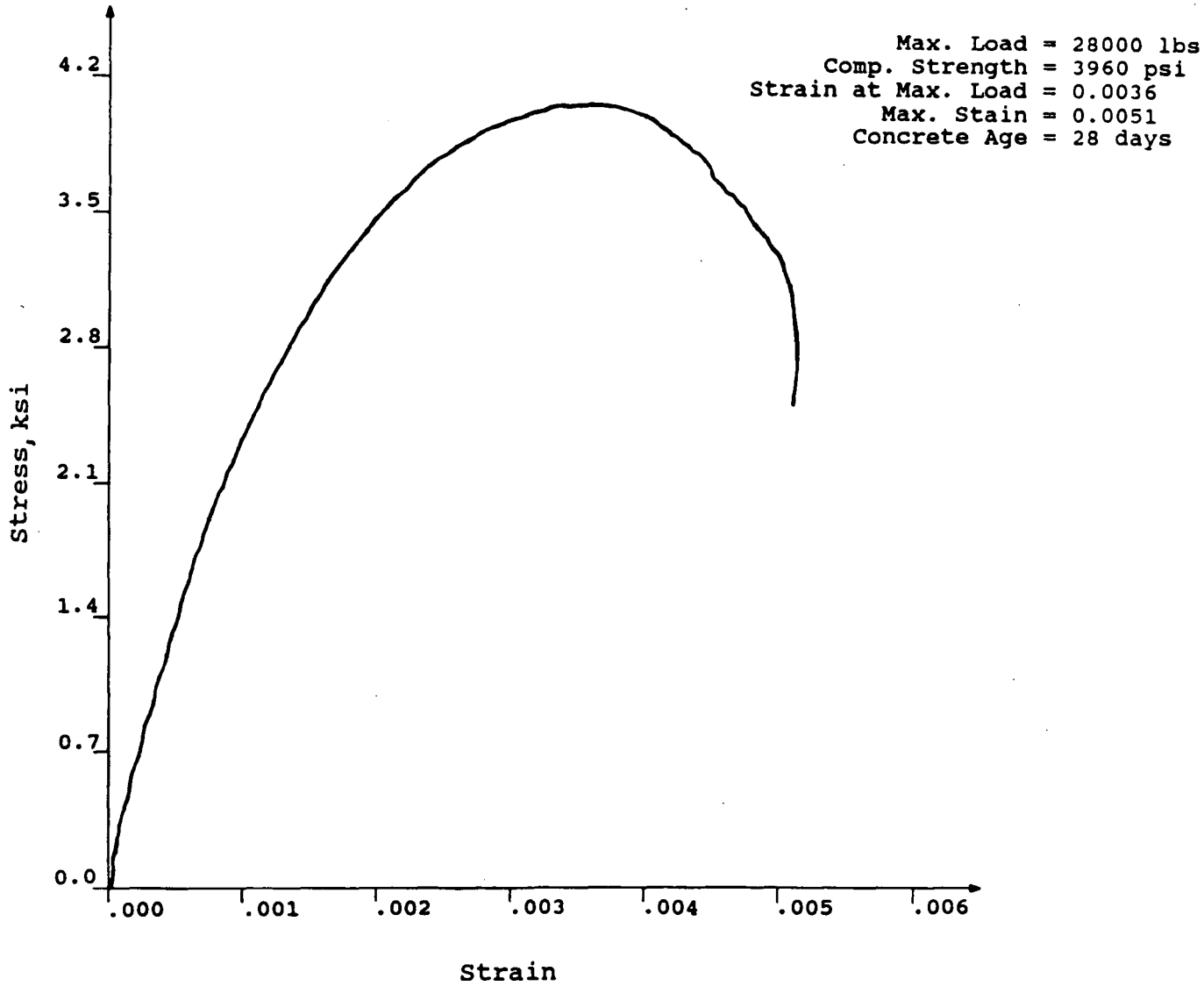

Figure 4-1: Stress-Strain Curve of Concrete

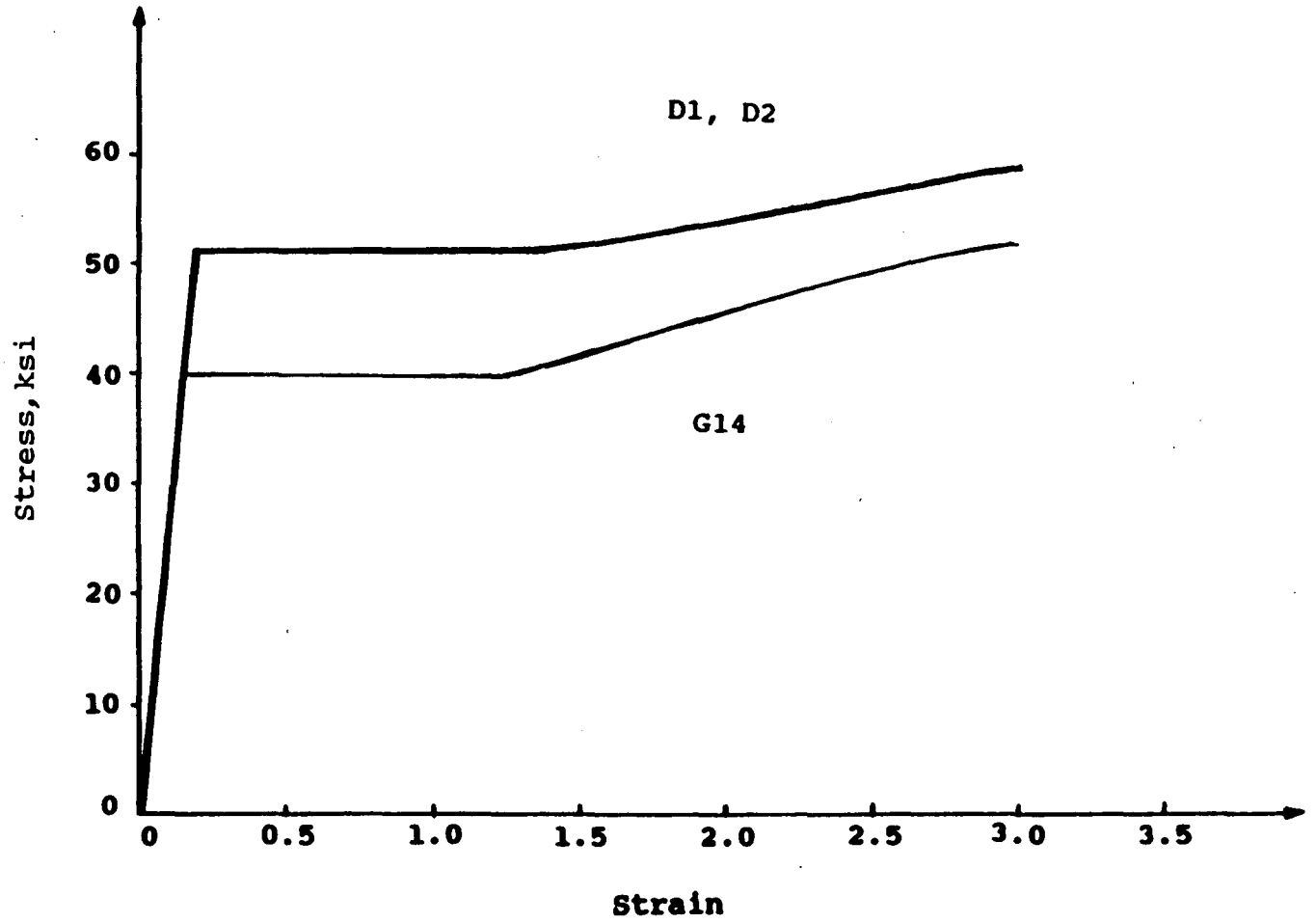

Figure 4-2: Stress-Strain Curves of D2, D1 and G14

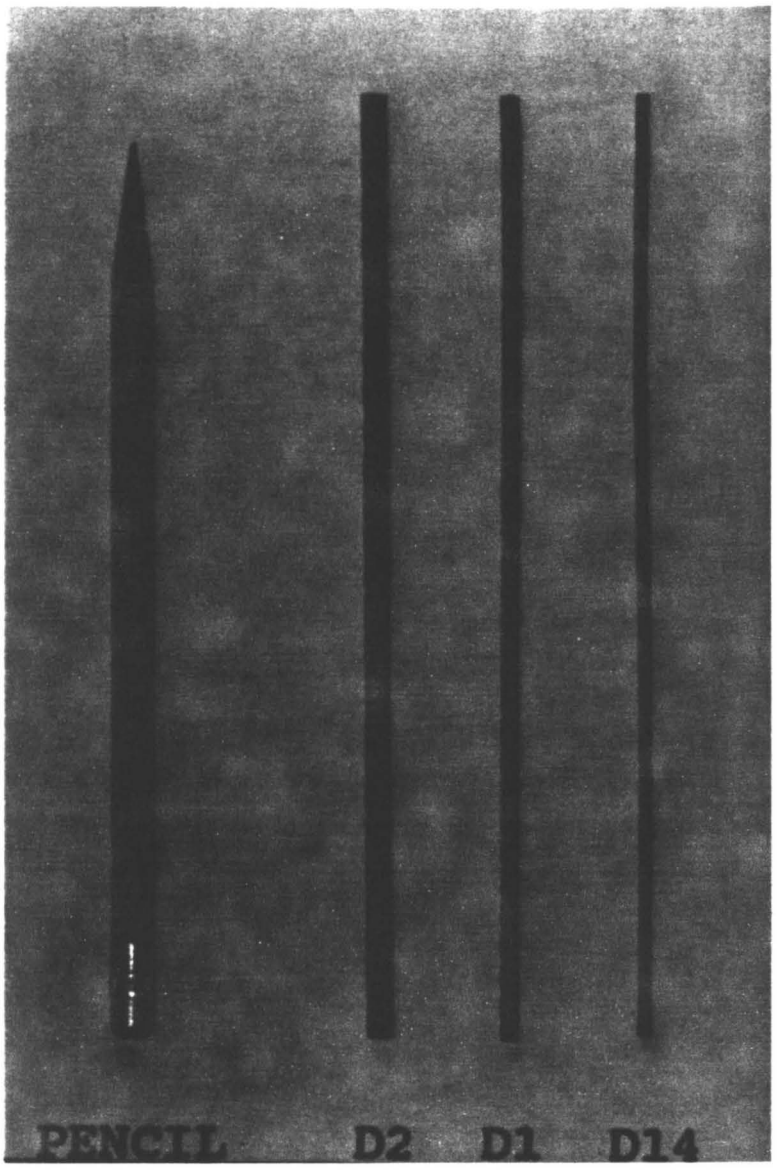

Figure 4-3: Deformed D2, D1 and G14

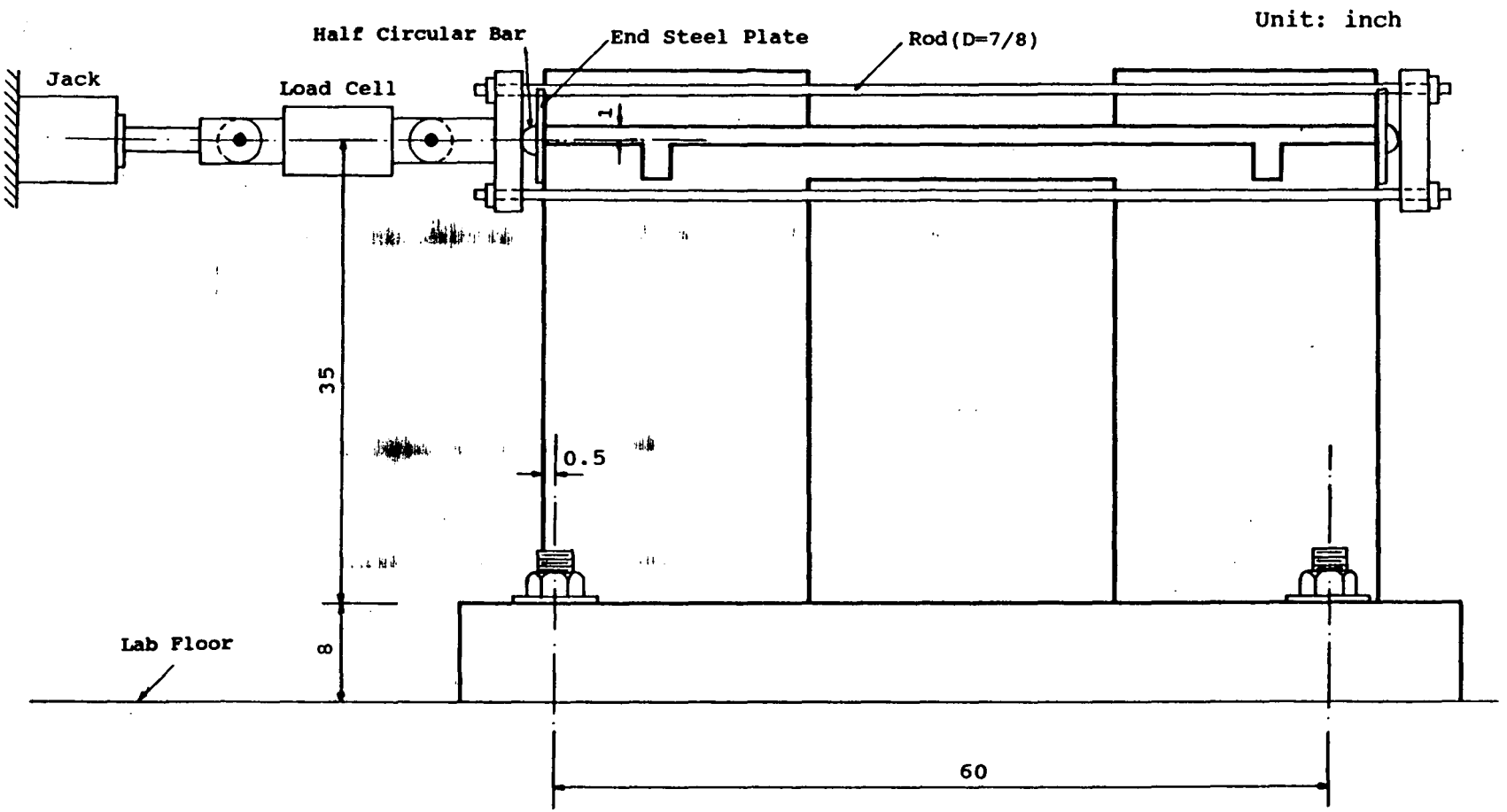

Figure 4-4: Test Setup for Shear Wall

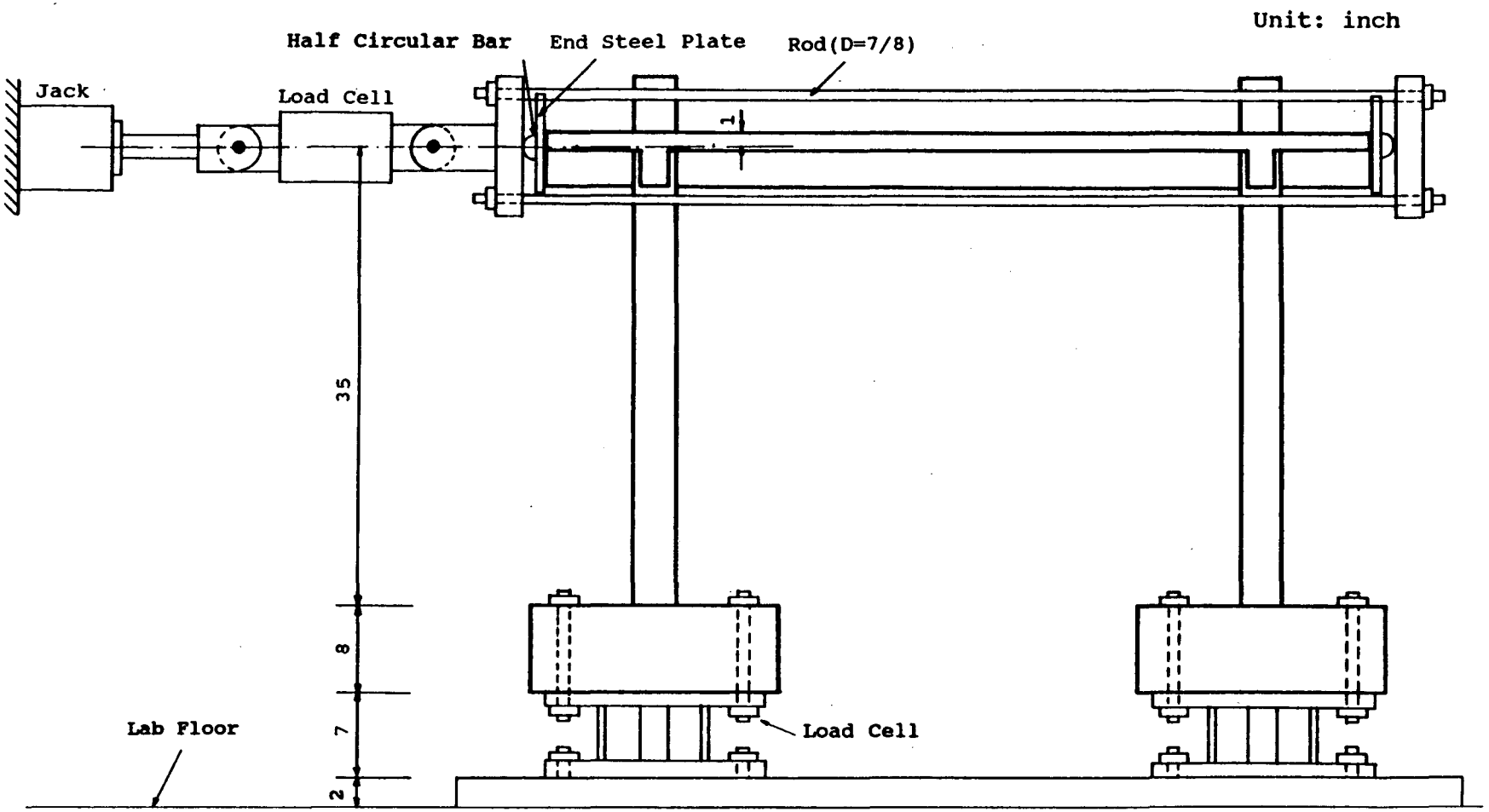

Figure 4-5: Test Setup for Frame

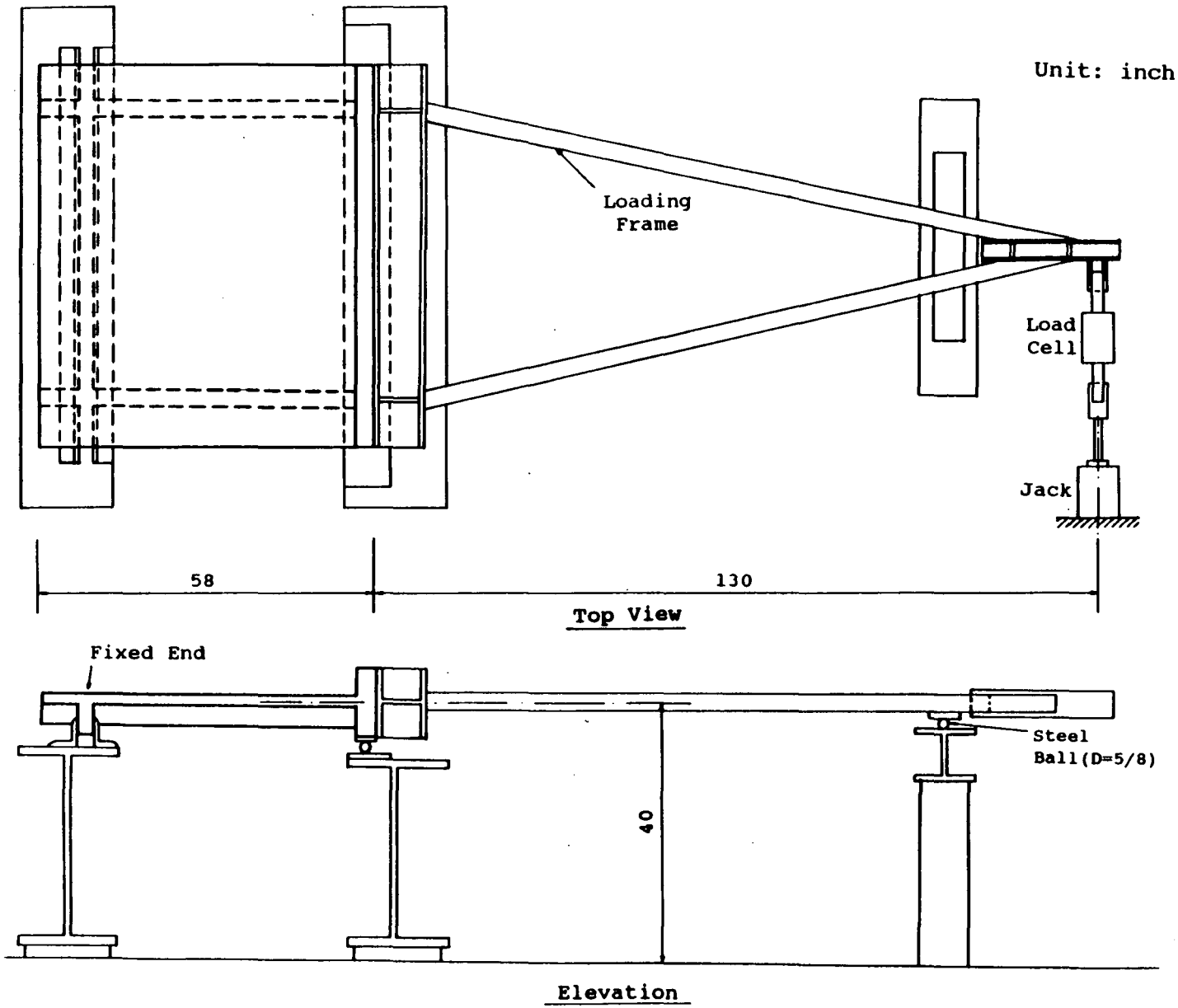

Figure 4-6: Test Setup for Slab

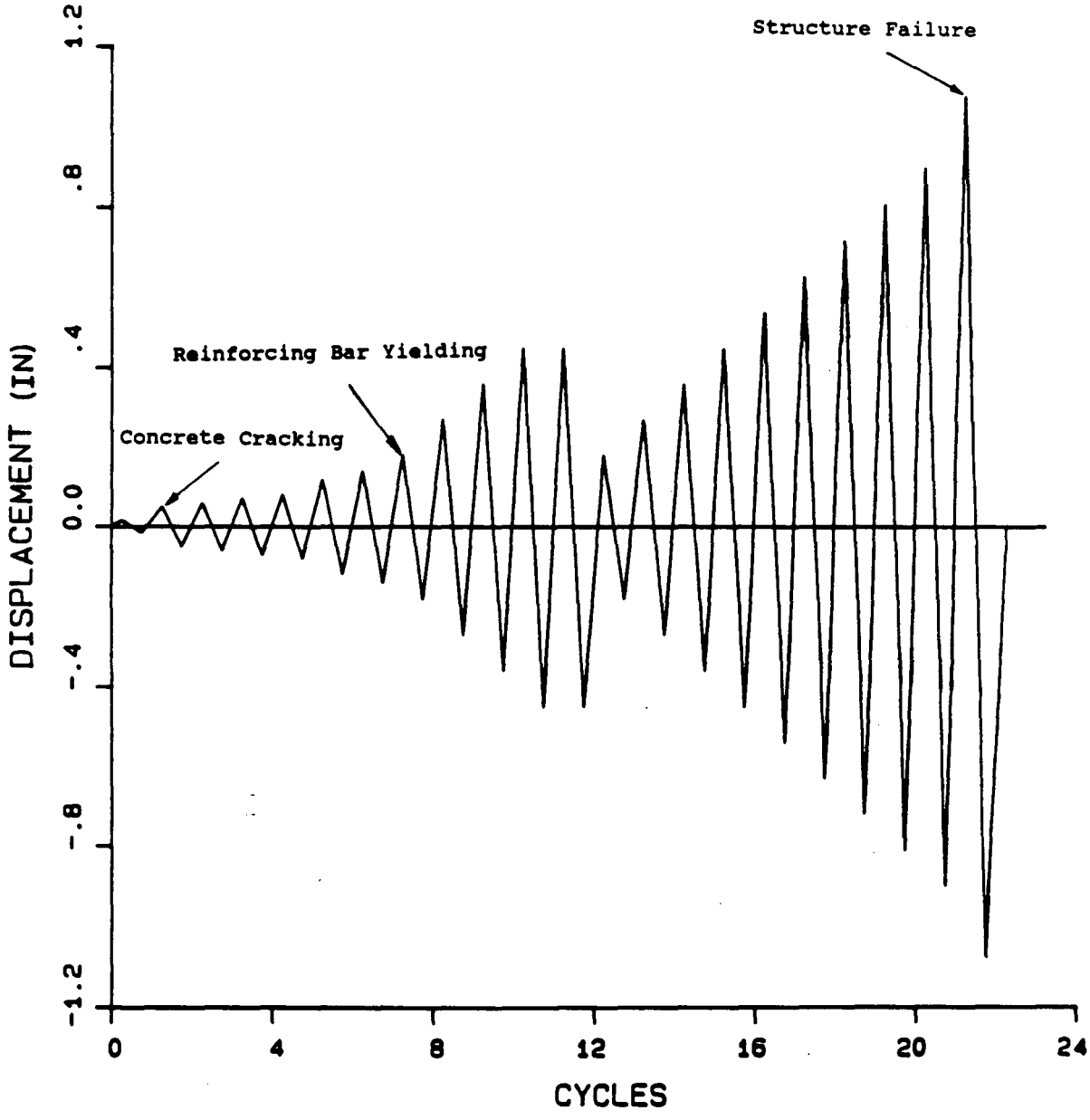

Figure 4-7: Loading Program for Shear Wall

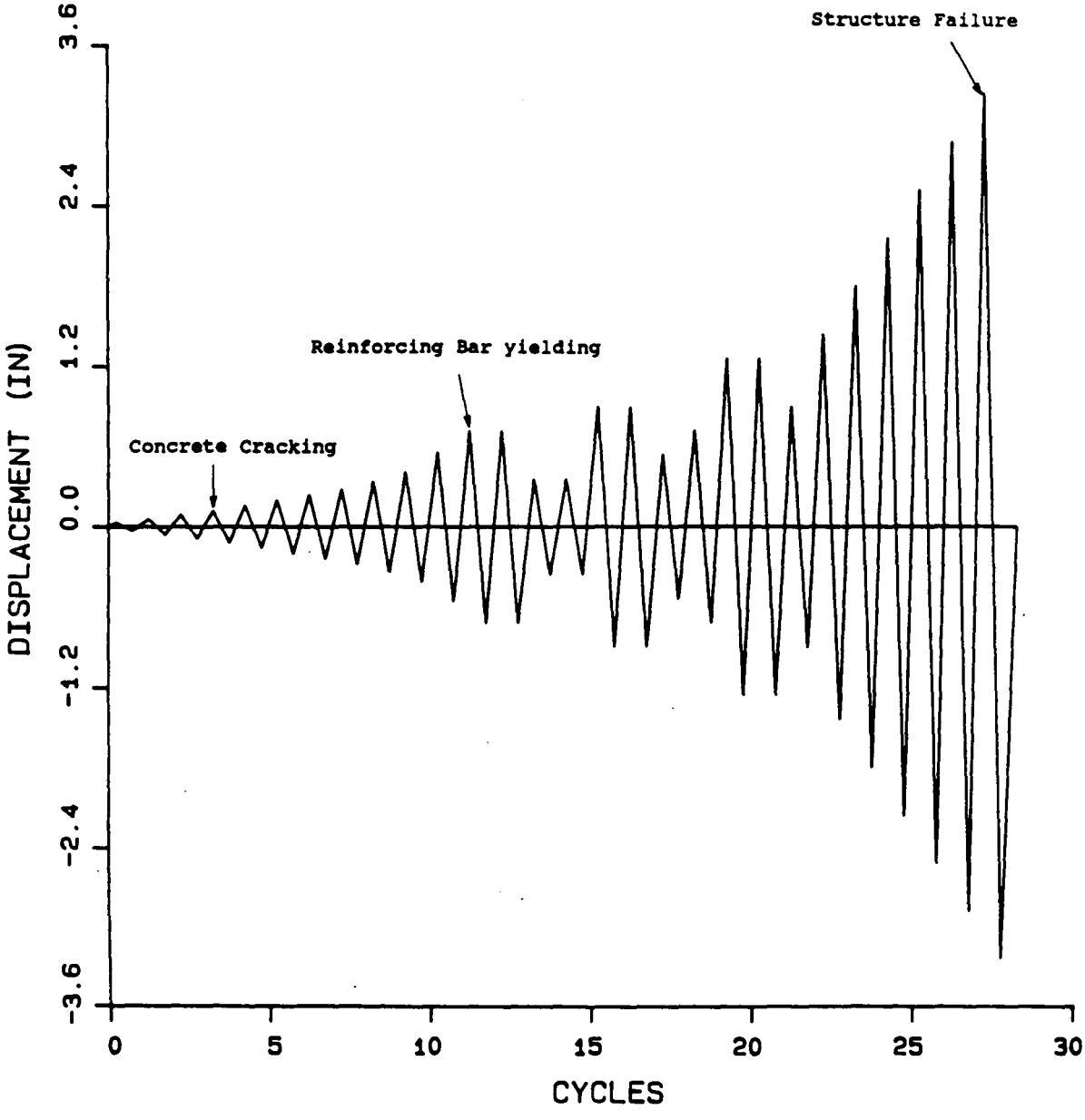

Figure 4-8: Loading Program for Frame

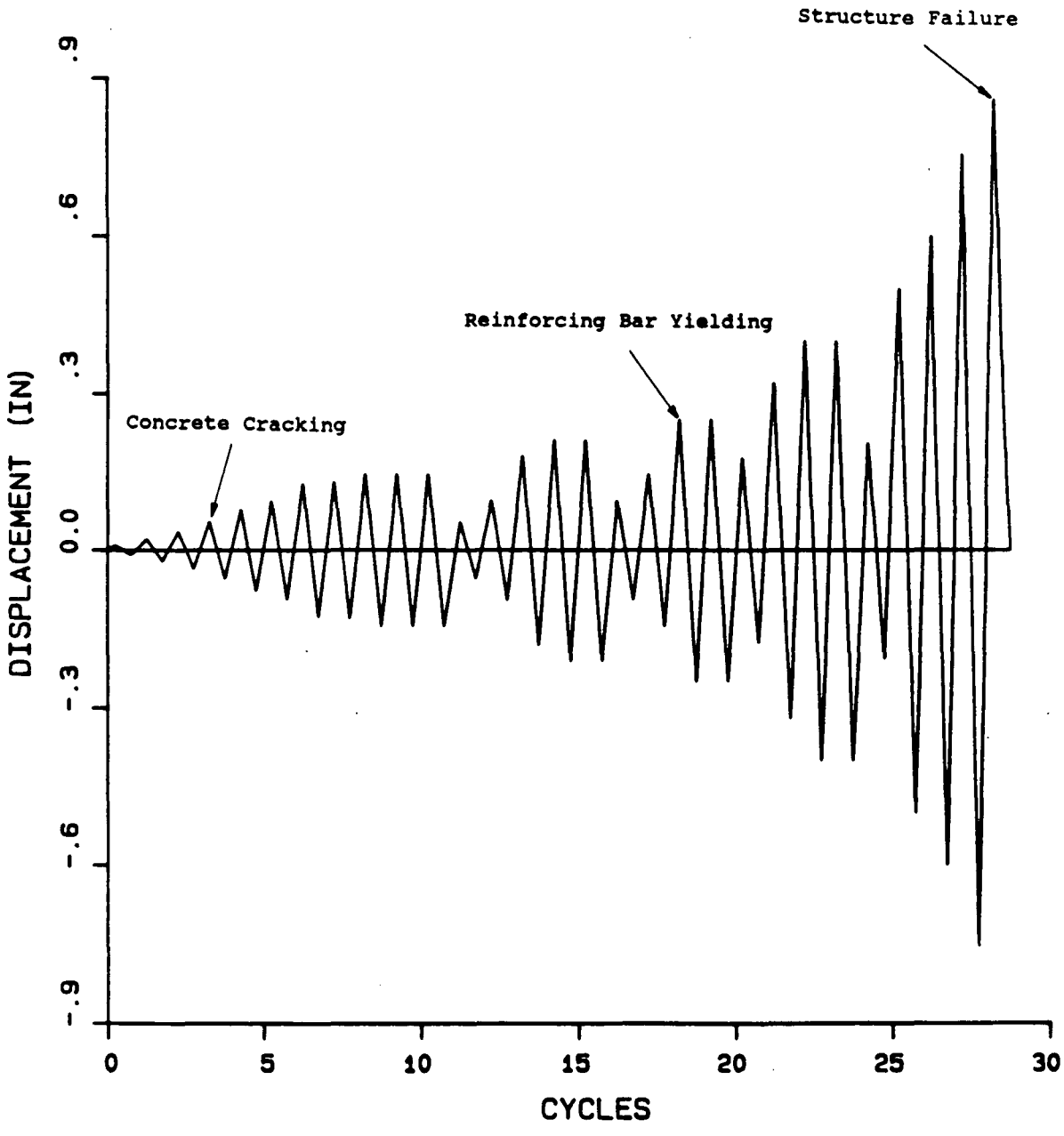

Figure 4-9: Loading Program for Slab

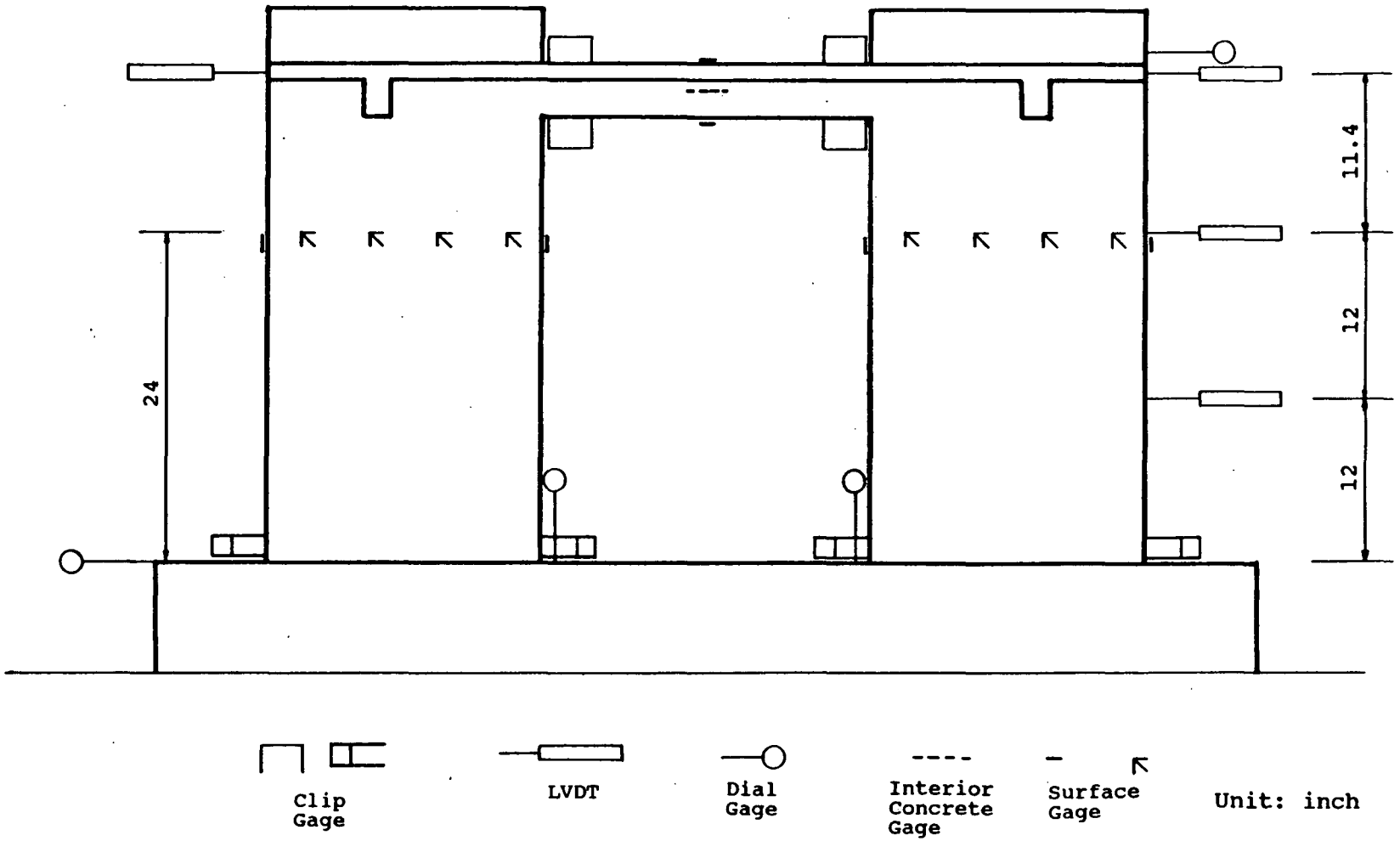

Figure 4-10: Instrumentation for Shear Wall

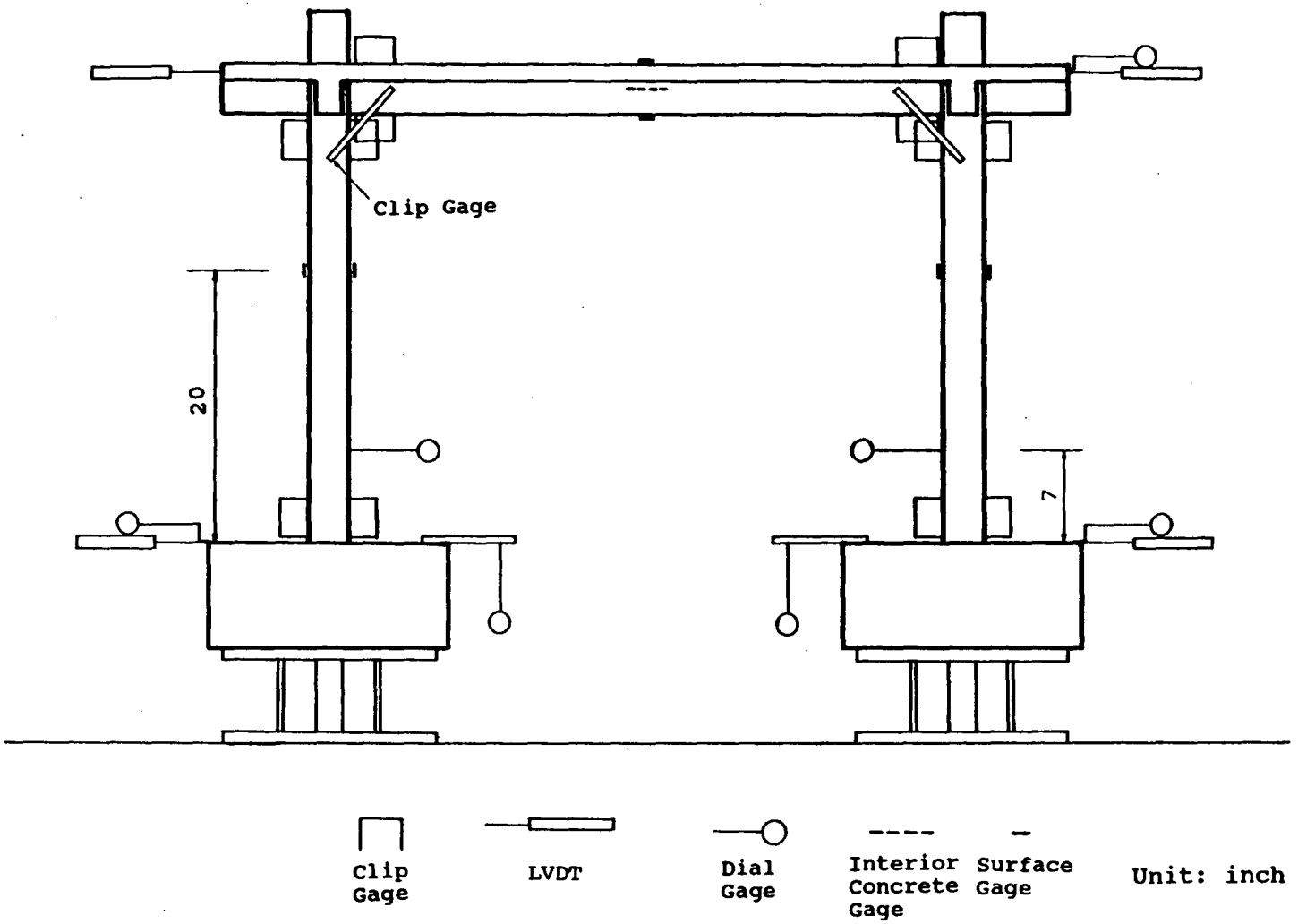

Figure 4-11: Instrumentation for Frame

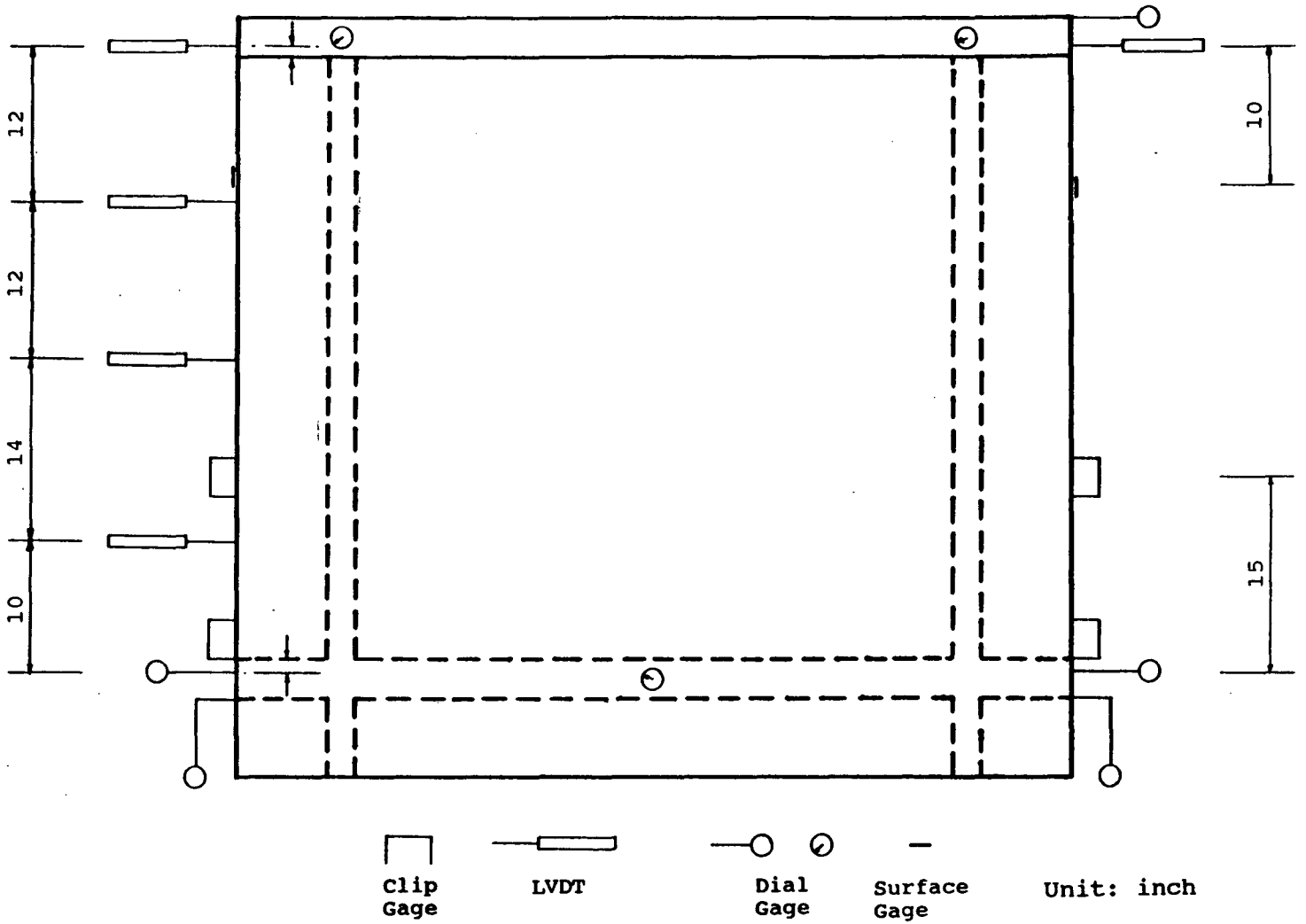

Figure 4-12: Instrumentation for Slab

Chapter 5
Summary

An one-story one-sixth scale reinforced concrete structure consisting of shear walls, frames and floor diaphragms has been developed to be the test structure in this study. The objective of the analytical and experimental study on the test structure is to investigate the seismic behavior of 3D reinforced concrete buildings at or near collapse with emphasis on diaphragm action and to correlate the theoretical predicted response with experimental observations.

The dynamic modelling requirements of the test structure are achieved by using the same material properties for both prototype and model structures and adding gravity load to compensate for the reduced effect of structural mass in the model. The design of the model structure was completed in accordance with ACI 318-83, including the special provisions for seismic design (Appendix A of ACI 318-83). Identical model assemblage structure will be used for the shaking table test at SUNY/Buffalo and the quasi-static test at Lehigh University. The three component specimens have been designed such that their testing results will contribute to more accurate predictions of the substructural behaviors of the assemblage tests at both Universities.

The ultimate strengths of the three components and the assemblage, obtained from the IDARC program analyses, are nearly the same as the design values. In the seismic response studies, the IDARC program also revealed some information about the hysteretic behavior of the model structures in inelastic range.

References

(1) ***Building Code Requirements for Reinforced Concrete***
American Concrete Institute, ACI 318-83, Detroit, 1983.

(2) Askar, G. and Lu, L.W.
Design Studies of the Proposed Six-Story Steel Test Building.
Research Report No. 467.3, Fritz Engineering Laboratory, Lehigh University, Bethlehem, Pennsylvania, 1985.

(3) Bathe, K.J., Wilson, E.L. and Peterson, F.E.
SAP IV: A Structural Analysis Program for Static and Dynamic Response of Linear Systems
University of California, Berkeley, June, 1973.

(4) Chen, S.J.
Reinforced Concrete Floor Slabs Under In-Plane Monotonic and Cyclic Loading.
PhD dissertation, Lehigh University, Bethlehem, Pennsylvania, 1986.

(5) Gonzalez, C., Lu, L.W. and Huang, T.
Seismic Damage Analysis of the Imperial County Services Building.
Research Report No. 422.12, Fritz Engineering Laboratory, Lehigh University, Bethlehem, Pennsylvania, December, 1983.
presented at the annual meeting of the Earthquake Engineering Research Institute, Santa Barbara, California, Feb. 1981.

(6) Jain, S.K.
Continuum Models for Dynamics of Buildings.
Journal of Engineering Mechanics, ASCE Vol. 110, No. 12:pp. 1713-1730, December, 1984.

(7) Jain, S.K. and Jennings, P.C.
Analytical Models for Low-Rise Buildings With Flexible Diaphragms.
Journal of Earthquake Engineering and Structural Dynamics Vol. 13, No. 2:pp. 225-241, March-April, 1985.

(8) Ji, X.R., Huang, T., Lu, L.W. and Chen, S.J.
An Experimental Study of The In-Plane Characteristics of Waffle Slab Panels.
Research Report No. 481.3, Fritz Engineering Laboratory, Lehigh University, Bethlehem, Pennsylvania, 1985.

(9) Karadogan, H.F. Huang, T., Lu, L.W. and Nakashima, M.
Behavior of Flat Plate Floor Systems Under In-Plane Seismic Loading.
In . 7th World Conference on Earthquake Engineering, Proceedings, Vol.5, pp. 9-16, Istanbul, Turkey, 1980.

(10) Krawinkler, H. and Moncarz, P.D.
Similitude Requirements for Dynamic Models.
Dynamic Modelling of Concrete Structures, ACI SP-73:pp. 1-15, 1982.

(11) Lee, S.J.
Seismic Behavior of Steel Building Structures with Composite Slabs.
PhD Dissertation, Lehigh University, Bethlehem, Pennsylvania, 1987.

(12) Nakashima, M., Huang, T. and Lu, L.W.
Seismic Resistance Characteristics of Reinforced Concrete Beam-Supported Floor Slabs in Building Structures.
Research Report No. 422.9, Fritz Engineering Laboratory, Lehigh University, Bethlehem, Pennsylvania, April, 1981.

(13) Nakashima, M., Huang, T. and Lu, L.W.
Experimental Study of Beam-Supported Slabs Under In-Plane Loading.
Journal of the American Concrete Institute Vol. 79, No. 1:pp. 59-65, January-February, 1982.

(14) Nakashima, M., Huang, T. and Lu, L.W.
Effect of Diaphragm Flexibility on Seismic Response of Building Structures.
In . 8th World Conference on Earthquake Engineering, Proceedings, Vol. IV, pp. 735-742, San Francisco, 1984.

(15) Park, Y.J., Reinhorn, A.M. and Kunnath, S.K.
IDARC:Inelastic Damage Analysis of Reinforced Concrete Frame-Shear-Wall Structures.
Technical Report NCEER-87-0008, National Center for Earthquake Engineering Research, State University of New York at Buffalo, July 20, 1987.

(16) Reinhorn, A.M., Kunnath, S.K. and Panahshahi,N.
Modeling of R/C Building Structures with Flexible Floor Diaphragms(IDARC2).
Technical Report NCEER-87-0035, National Center for Earthquake Engineering Research, State University of New York at Buffalo, September 7, 1987.

(17) Shen, S.Z. and Lu, L.W.
Substructure Analysis of Multistory Buildings with Flexible floor.
Research Report No. 422.13, Fritz Engineering Laboratory, Lehigh University, Behtlehem, Pennsylvania, 1985.

(18) ***Uniform Building Code***
1982 edition, International Conference of Building Officials, California, 1982.

(19) Wakabayashi, M.
Design of Earthquake-Resistant Buildings.
McGraw-Hill, New York, New York, 1986.

(20) Wang, C.K. and Salmon, C.G.
Reinforced Concrete Design.
4th Edition, Harper & Row, New York, New York, 1985.

(21) Wilby, G.K., Park, R. and Carr, A.J.
Static and Dynamic Loading Tests on Two Small Three-Dimensional Multistory Reinforced Concrete Frames.
Dynamic Modelling of Concrete Structures, ACI SP-73:pp. 35-64, 1982.

(22) Wu, Z.S. and Huang, T.
An Elastic Analysis of a Cantilever Slab Panel Subjected to an In-Plane End Shear.
Research Report No. 481.1, Fritz Engineering Laboratory, Lehigh University, Bthelehem, Pennsylvania, 1983.

Appendix A
Seismic Load Calculation

Seismic load V = cW, c = ZIIIKCS, Z = III = 1 and W = 487.3 kips

Transverse direction(along Frame B)

T = 0.04 sec.

S = 1.5

K = 0.8

C = 0.12

CS = 0.18>0.14 use 0.14

c = 0.112

V = 0.112W = 54.6 kips

Longitudinal direction(along Frame A)

T = 0.3 sec.

S = 1.5

K = 0.67

C = 0.12

CS = 0.18>0.14 use 0.14

c = 0.094

V = 0.094W = 45.7 kips